Imaging mass spectrometry for metabolites: Technical progress, multimodal imaging, and biological interactions

Article *in* Wiley Interdisciplinary Reviews Systems Biology and Medicine · May 2017

DOI: 10.1002/wsbm.1387

CITATIONS
5

READS
577

3 authors, including:

Ying-Ning Ho
Academia Sinica
15 PUBLICATIONS **161** CITATIONS
SEE PROFILE

Yu-Liang Yang
Academia Sinica
92 PUBLICATIONS **2,123** CITATIONS
SEE PROFILE

Advanced Review

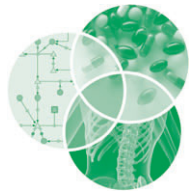

Imaging mass spectrometry for metabolites: technical progress, multimodal imaging, and biological interactions

Ying-Ning Ho,[†] Lin-Jie Shu[†] and Yu-Liang Yang*

Imaging mass spectrometry (IMS) allows the study of the spatial distribution of small molecules in biological samples. IMS is able to identify and quantify chemicals *in situ* from whole tissue sections to single cells. Both vacuum mass spectrometry (MS) and ambient MS systems have advanced considerably over the last decade; however, some limitations are still hard to surmount. Sample pretreatment, matrix or solvent choices, and instrument improvement are the key factors that determine the successful application of IMS to different samples and analytes. IMS with innovative MS analyzers, powerful MS spectrum databases, and analysis tools can efficiently dereplicate, identify, and quantify natural products. Moreover, multimodal imaging systems and multiple MS-based systems provide additional structural, chemical, and morphological information and are applied as complementary tools to explore new fields. IMS has been applied to reveal interactions between living organisms at molecular level. Recently, IMS has helped solve many previously unidentifiable relations between bacteria, fungi, plants, animals, and insects. Other significant interactions on the chemical level can also be resolved using expanding IMS techniques.

How to cite this article:
WIREs Syst Biol Med 2017, e1387. doi: 10.1002/wsbm.1387

INTRODUCTION

Metabolites play important roles in maintaining life (primary metabolites for growth, development, and reproduction) and in ecological functions (secondary metabolites for antibiotics and pigments). To gain insight into complicated interactions (e.g., molecule distribution, exchange, and transportation) in biological processes that have temporal variation requires new technologies and approaches. Using modern analytical techniques, such as liquid chromatography-mass spectrometry (LC-MS) and liquid chromatography-nuclear magnetic resonance (LC-NMR), it is possible to dereplicate or identify some molecules when interactions occur at a specific time or under a specific condition. And, in combination with genomic and transcriptomic information, we have an opportunity to explore and predict the molecules involved in chemical and biological interactions.[1–3] However, detailed molecular distribution and localization in biological samples is still difficult to elucidate because of technical limitations.

Imaging mass spectrometry (IMS) fills a niche in the evaluation and identification of molecules *in situ*, from complex samples to single cells, and from biological macromolecules to small metabolites. Although there have been remarkable advances in IMS, some technical limitations are still hard to surmount, particularly with regard to small molecule (metabolite) analysis. Sample preparation and

[†]These authors contributed equally to this work.

*Correspondence to: ylyang@gate.sinica.edu.tw

Agricultural Biotechnology Research Center, Academia Sinica, Taipei, Taiwan

Conflict of interest: The authors have declared no conflicts of interest for this article.

instrument improvement are the key components for successful application of IMS to the analysis of various biological samples and analytes. Several outstanding reviews have introduced different aspects of IMS such as advances in vacuum ionization[4–6] and ambient ionization.[7,8] In addition, reviews about the application of IMS in histology,[9,10] pathology,[11,12] pharmaceutical science,[13,14] plant science,[15–18] microbiology[19–21] and so on have detailed the value and advantages of the IMS-based workflow. To complement those works, in this review, we focus on recent developments in the use of IMS for metabolite analysis, focusing specifically on technological advancement and their applications. First, we introduce several new technical advances, such as sample preparation approaches, hardware improvement, and the development of qualitative and quantitative approaches. Then we look at recent applications such as multimodal imaging systems, and discuss current challenges and future perspectives for applying IMS to answer different biological questions.

Challenges and breakthroughs in IMS are introduced in the two sections entitled '*Vacuum Ionization Imaging Mass Spectrometry Systems*' and '*Ambient Ionization Imaging Mass Spectrometry Systems*.' With innovative MS analyzers, powerful MS spectral databases, and analysis tools, IMS is capable of aiding the 'dereplication' of known metabolites, that is, the rapid identification of known compounds, and even identification of unknown metabolites. In the section entitled '*Metabolite Identification and Quantification*,' current approaches for metabolic identification and quantification are detailed. IMS can also assist classical analytical methods with chemical information when coupled with other popular imaging techniques such as fluorescence microscopy. We introduce some multimodal imaging systems together with examples of their application in the section entitled '*Multimodal imaging systems*.' Nowadays, cutting-edge research often utilizes IMS to unravel tricky biological problems. IMS can be used to investigate complicated interactions between species at the small molecular level. In recent years, IMS has been used to demonstrate many relationships between bacteria, fungi, plants, animals, and insects. In addition, other crucial interactions at the chemical and even molecular levels can be answered by rapidly expanding IMS-based research. Such applications are described and discussed in the section entitled '*Application of IMS in Biological Interactions*.' This review mainly covers research published recently, since 2014. For IMS basic principles and technical protocols, readers are kindly referred to the IMS e-books on those topics listed in 'Further reading.'

VACUUM IONIZATION IMAGING MASS SPECTROMETRY SYSTEMS

Secondary ion mass spectrometry (SIMS), laser desorption/ionization (LDI), matrix-assisted laser desorption/ionization (MALDI), and surface-assisted laser desorption/ionization (SALDI) IMS are vacuum imaging mass spectrometry techniques that are widely performed on axial time-of-flight (TOF) instruments.[22–24] TOF-SIMS was one of the first mass spectrometry techniques applied to IMS. To date, TOF-SIMS has been used to study biomolecular distribution of surfaces or subsurfaces such as human tissues (breast tumor,[25] glioblastoma cells,[26] and neuronal cells[27]), microbes,[28] and nematodes.[29] Because of the high spatial resolution (~nm) in TOF-SIMS-IMS, it is capable of analyzing molecular distribution at the single-cell level.[30] MALDI-IMS is the most versatile IMS technique for application in plant tissues,[31] animal tissues,[13] cancer cells,[32] and microbial communities,[33,34] especially macrobiomolecules such as peptides and proteins. However, for small molecule detection, organic matrix signals interfered with the detection for analytes below 600 Da. Therefore, the matrix-free LDI-MS is an alternative technique for the profiling and imaging of small molecules. The distributions of secondary metabolites of *Arabidopsis thaliana* and *Hypericum* species were demonstrated by using LDI-IMS in negative mode.[35] However, LDI-MS is only applicable to molecules with chromophores. To counter these problems, many inorganic nanomaterials have been developed as substrates for SALDI-MS.[36–38] SALDI-MS has been developed to allow a wide mass range of proteins, peptides,[39] carbohydrates,[40] and small metabolite analysis in IMS. In all the aforementioned IMS experiments, sample preparation is the most critical process for collecting high-quality data. Several studies to address the typical problems of vacuum ionization IMS (e.g., inhomogeneous matrix deposition, matrices interference, and narrow mass range) have made significant strides recently. In this section, we focus on the current development of MALDI-IMS, SALDI-IMS, and SIMS-IMS.

MALDI-IMS

The MALDI is widely used for the detection of analytes from sample surface. The focused infrared (typical wavelengths 2.94 or 10.6 μm) or ultraviolet (UV) (337, 355, or 266 nm) laser beam is used as an irradiation source of MALDI or LDI-MS. In MALDI-MS, the analytes are cocrystallized with organic or inorganic matrix, which helps release the

analytes into the gas phase in a process leading to ionization and enhancing the intensity of analytes. As the matrix can absorb the energy of the UV laser beam showing little fragmentation in the mass spectra, MALDI is considered to be a soft ionization technique. Commercial MALDI-MS spectrometers equipped with UV laser beams are offering spatial resolutions of around 20 μm,[41] although in a few cases higher resolution of around a few microns (up to single cell) have been presented.[42] However, the size of the matrix and analyte cocrystals should be smaller than the required lateral resolution of the imaging experiment. Infrared LDI (IR-LDI) simply uses the endogenous water or frozen solvents as a matrix that enables the direct detection of a wide range of molecules without further matrix compounds. IR-LDI IMS of biological tissue with a spatial resolution of 30 μm has recently been reported.[43] IR-LDI IMS can directly image the samples in their natural state, but a point of concern is that the evaporation of water causes a severe reduction in the ion yield during the long acquisition on an image. Furthermore, a fairly homogenous distribution of water in the sample is not necessarily met in all samples with the use of physiological water as matrix. In addition, the disadvantage of IR-LDI is that infrared laser radiation is much more difficult to focus than UV. UV laser radiation spot size can easily be focused to one micrometer in comparison to IR lasers for which the limit is around 30 μm.[44]

Matrix Deposition Approach

The size of matrix-analyte cocrystals is strongly correlates with MALDI-IMS data quality.[45] The matrices are deposited using several methods including liquid spraying, dry coating, and sublimation. For moist samples, such as microbes cultured on the agar media, application of solid matrices prior to sample dehydration using a stainless steel sieve is an efficient, low-cost, and widely used method for uniform dry-coating.[21] Automatic matrix deposition methods for supplying homogeneous matrix have been demonstrated in previous studies by using commercial instruments such as ImagePrep (Bruker) and HTX TM-Sprayer (HTX Technologies) or self-made sprayers. A robotic sprayer for matrix application was used to provide a significant increase in MALDI-IMS sensitivity compared with the sieve method.[46] Nebulized matrix solutions can be homogeneously applied onto wet and dried agar to result in better sensitivity for specific metabolites.[47,48]

For tissue samples, sublimation allows fast and uniform dry matrix deposition.[49] The tissue sample was placed and inverted over the top of the matrix in a sublimation chamber. The solid matrices are amenable to sublimation at elevated temperatures and reduced pressure while the sample attached to the cold-finger remains cooled. The advantages of this process include the desired effect of purifying the matrix and forming fine crystals for high spatial resolution IMS.[50] Sublimation is a solvent free process; therefore, the extraction efficiency is poor for some molecules. Additional rehydration is suggested to improve extraction efficiency and then increase sensitivity.[51] The technique has been demonstrated for imaging lipids[45] and small molecules.[52] The comparison of these matrix deposition methods is showed in Figure 1(a). Another matrix spraying method, the electric field-assisted matrix coating method (EFASS) has been developed to enhance the detection of small metabolites in tissue samples.[48] The EFASS matrix coating system generates homogeneous crystals with a size of less than 10 μm and gives excellent signal intensities and number of detected metabolites in tissue, compared with sublimation and sieving matrices.[53]

Recently many homemade systems have been built for easily generating homogenous and small matrix crystals on the samples,[47] leading to improve detection and imaging quality of small metabolites. Suitable techniques can be selected to improve matrix deposition for MALDI-IMS depending on the target samples.

Matrix Choices

The detection of specific molecules in MALDI-IMS is highly dependent on the choice of matrix. The matrix is essential for ionizing the analytes and then improving the sensitivity of MALDI-IMS. Commercial matrices such as 2,5-dihydroxybenzoic (DHB) acid and cyano-4-hydroxycinnamic acid (CHCA) are common choices for MALDI-IMS. However, the matrix or matrix-analyte cluster signals always interfere with small molecule detection. Recently, several studies have made significant progress in the development of novel matrices for small molecules, such as nanomaterials[54] and organic matrices 2,3,4,5-tetrakis (3′,4′-dihydroxylphenyl)thiophene (DHPT),[55] 1-naphthylhydrazine hydrochloride (NHHC),[56] *N*-(1-naphthyl)ethylenediamine dinitrate (NEDN),[57] and 1,5 naphthalenediamine (1,5-DAN).[58] DHPT was designed for the analysis of small molecular amines in positive ion mode.[55] NHHC, the ideal salt-tolerant matrix, was selected to monitor glucose in serum with high sensitivity and homogentisic acid in urine was detected in negative ion mode.[56] An organic salt NEDN has been employed to analyze oligosaccharides, peptides, and metabolites in negative mode.[57]

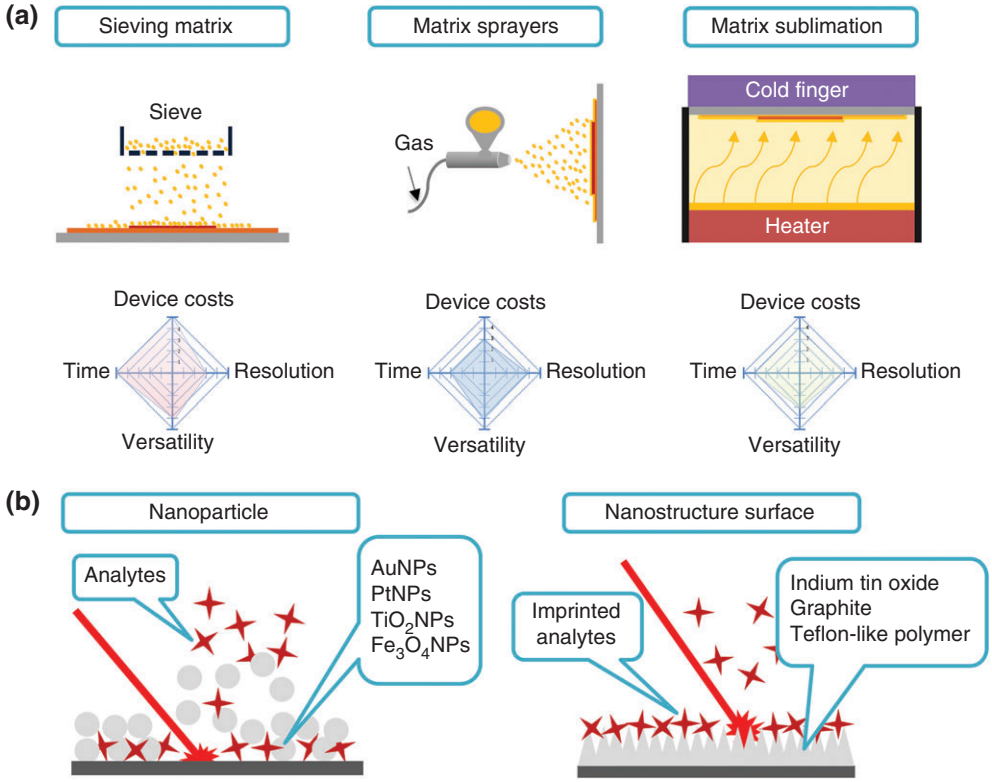

FIGURE 1 | Schematic overview of matrix deposition approaches for a matrix-assisted laser desorption ionization (MALDI)-time-of-flight (TOF)-Imaging mass spectrometry (MS) platform. (a) Sieving matrix, matrix sprayers, and matrix sublimation were evaluated according to device cost, time (matrix deposition time-consumption), versatility (sample types, and matrix choices), and resolution (increasing signal efficiency and matrix crystallite size). After comparison of these three deposition methods, the top 1 was assigned a score of 5, followed by scores of 4 and 3 for the next positions. We chose commercial matrix sprayers (ImagePrep and HTX TM-Sprayer) as candidates for evaluating with other methods. (b) Schematic overview of nanomaterial substrates and nanostructural-coated slides on a surface-assisted laser desorption/ionization (SALDI) imaging MS system. The cross symbols represent analytes.

NEDN was designed with properties of a strong UV absorbing chromophore and nitrate anion donors to provide a significant improvement in sensitivity and yielded few matrix-associated interferences compared with DHB and CHCA. NEDC-assisted LDI-IMS was applied to a mouse model of colorectal cancer liver and yielded more endogenous metabolites (ranging from *m/z* 60 to 1600) than 9-aminoacridine for analysis of multiple glycerophospholipids, glucose, and other small metabolites.[32] The newly prepared matrix 1,5-DAN hydrochloride was applied in mouse liver, brain, and kidneys.[58] 1,5-DAN has the advantages of low cost, strong UV absorption, high salt tolerance capacity and provides fewer background signals in the low mass range allowing us to visualize the spatial distribution of amino acids, nucleotide derivatives, peptide, lipids, and carboxylic acids. 1,8-Bis(dimethylamino)naphthalene (DMAN), an ionless matrix, does not produce matrix interference for small molecule analysis.[59] However, it is unstable under high vacuum conditions.[60] This property causes matrix limitation while performing higher spatial resolution MALDI-IMS, which takes long time to scan the samples. In order to overcome the limitation of the amount of time needed, Potočnik reported a new type of axial MALDI-TOF instrument that uses a 10 kHz pulsed laser beam and two rotating mirrors to allow high spectral acquisition rate (up to 50 pixels/second).[61] This high-speed approach makes possible MALDI-IMS studies of new classes of unstable matrix under high vacuum.

SALDI-IMS

Several SALDI-MS techniques have been developed for small molecule detection in view of the problem of matrix interference in the low mass range (below 600 Da).[62,63] SALDI-MS has the advantages of low background signals, highly efficient ionization process, rapid analysis and easy sample preparation, and equivalent spatial resolution (~20 μm) in comparison with MALDI-MS.[64] Rowell, Hudson, and Seviour

demonstrated the first SALDI-IMS for metabolites and drugs from latent fingerprints.[65] Tang et al. used gold nanoparticles (AuNPs) to obtain optical images of the overlapping latent fingerprints and stearic acid and palmitic acid were detected.[66] These successes nicely highlight the potential of SALDI-IMS for revealing the spatial distribution of small molecules. A stamping (imprint) method for the detection of active precursors and common small metabolites (e.g., 6,6-dibromoindigo and tyrindoxyl sulfate) from marine mollusk tissue was demonstrated by performing desorption ionization on porous silicon (DIOS)-IMS.[67] Nanostructured laser desorption ionization (NALDI)-IMS has been performed using the same approach.[68] However, some molecules that were detected by NALDI-IMS were not observed by DIOS-IMS. A similar phenomenon was also found in AuNP-IMS and TiO_2NP-IMS. AuNP IMS could generate clean mass spectra, but many molecules that were seen in TiO_2NP-IMS were not observed.[69] These findings suggest that variations of surface functionalization and nanostructures might be exploited for detection of different small metabolites. Furthermore, Rudd et al. demonstrated a derivative application of the stamping or imprint method for SALDI-IMS; the use of 'on-surface' solvent separation of metabolites from tissue imprints for NALDI and DIOS-IMS.[70] This process allowed solvent extraction of subsets of metabolites according to polarity, directly from marine mollusk onto NALDI and DIOS surfaces for IMS to collect qualitative and relative quantitative data. Nanostructure initiator mass spectrometry (NIMS) is also a matrix-free platform that requires minimal sample preparation and has advantages in detection of small molecules with low background noise. NIMS-IMS has been applied for *in situ* kinetic histochemistry,[71] characterization of microbial interactions,[72] monitoring metabolites in rat brain sections,[73] and analyzing protein–metabolite interactions.[74]

Nanomaterial Substrate and Coated Slides

SALDI substrates generally consist of metal-based, carbon-based, and semiconductor-based materials. Several micro and nanomaterials (Au, Ag, graphite, and magnetic NPs) have been used for the analysis of small molecules in SALDI-MS. SALDI-MS based on TiO_2 NPs was utilized to detect catechins, (–)epigallocatechin (EGC), (–)epigallocatechin gallate (EGCG), phospholipids (PLs), and triacyl-glycerides (TAGs) in tea and soybean samples.[75,76] Fe_3O_4 NPs and Pt NPs make it possible to analyze peptides and proteins through SALDI MS. Coating of the Fe_3O_4 NPs with the shell of SiO_2 allowed the detection of myoglobin (*m/z* 16 kDa).[77] Pt NPs were used for the detection of various biomolecules including angiotensin I (*m/z* 1298 Da), insulin (*m/z* 5807 Da) and cytochrome C (*m/z* 12,360 Da).[78] This approach provided better quality biopolymer mass spectra. To date, several novel nanostructured-coated slides have been developed for SALDI-IMS of small metabolites and drugs (Figure 1(b)). Commercial indium tin oxide (ITO) glass slides were applied as IMS sample plates to reveal the spatial distribution of metabolites in sample tissues.[79] de Laorden et al. displayed the specific preparation and custom-made ITO-coated glass slides by radio frequency magnetron sputtering.[24] Ozawa et al. employed a homogeneously sputter-deposited PtNP film for the analysis of glycerolipids in rat brain tissue.[80] Stopka et al. developed a new IMS technique using nanophotonic laser desorption ionization platforms on a highly uniform silicon nanopost array.[81] Hybrid nanoporous structure films with silver nanoparticles (AgNPs) and reduced graphene oxide (rGO) were used for the rapid analysis of small molecules,[82] although this AgNPs/rGo hybrid layer-by-layer film has not been applied in tissue IMS. It has great potential for increasing the sensitivity of numerous analytes on the surface of graphene-based substrates.

SIMS-IMS

TOF-SIMS with super high spatial and depth resolution is suitable for single-cell IMS analysis. Recently, new TOF-SIMS techniques and strategies have been developed and applied in various biological fields (bacterial biofilm and animal tissues). Hua et al. reported the first *in situ* molecular imaging of a hydrated biofilm by using a microfluidic reactor and a TOF-SIMS application.[83] Park et al. analyzed cancer and adjacent normal tissues by using a multidimensional SIMS approach that combines metal-assisted SIMS and conventional TOF-SIMS.[84] Tian et al. showed that doping a small amount of CH_4 into the Argon cluster enhances the ionization of several biological molecules.[85] Compared to MALDI-MS, a focused high-energy primary ion beam (e.g., Ga+, In+, Ar+) is used to directly strike the sample surface for ionization in SIMS. The analyte molecules released from the surface are ionized upon collision with the primary ions without cocrystallization with matrix. As the high energy used in SIMS causes extensive secondary ion fragmentation, its mass range is limited to ~1.5 k Da (MALDI up to ~500 k Da).[86,87] The typical sample preparation of SIMS-IMS is similar to MALDI-IMS except for the matrix deposition. However, recent strategies are to

coat the sample surface with common MALDI matrices and metallization of samples with gold and silver to extend the potential of SIMS.[88,89]

Mass Resolution and Spatial Resolution Improvement

TOF-SIMS-IMS is a particularly useful method to map the various small molecules at the surface of biological samples. The TOF-SIMS focusing mode of the primary ion beam delivered by liquid metal ion cluster guns provides high spatial or high mass resolution. However, a combination of both high spatial and high mass resolution is commonly not possible. Burst Alignment (BA) mode and alternative high current bunched (HCBU) mode are two prominent ion beam focusing modes in TOF-SIMS. BA mode can provide submicrometer lateral resolution by using a pair of electrostatic lenses to produce a very narrow beam diameter. The disadvantage of this mode is a low current of primary ions that typically results in poor mass resolution. On the other hand, HCBU mode can provide high mass resolution by producing a primary ion buncher system. However, a large beam diameter caused moderate spatial resolution. Vanbellingen et al. developed a new method with delayed extraction by combining these two features resulting in both high mass and high spatial resolutions.[90]

AMBIENT IONIZATION IMAGING MASS SPECTROMETRY SYSTEMS

Ambient ionization mass spectrometry (AIMS) completes the ionization procedures under atmospheric pressure. Owing to little or no sample preparation and no matrix interference, AIMS has been another popular choice to present the spatial distribution of molecules *in situ* over the past 10 years.[91] Based on the ionization mechanism, AIMS is mainly divided into solid–liquid extraction methods and laser-assisted desorption methods.[92] Desorption electrospray ionization (DESI) is a widely-used solid–liquid extraction AIMS system applied in IMS and has been commercialized. Since 2007, several similar concepts and improvement in DESI techniques have been constructed for IMS,[93] such as nanospray desorption electrospray ionization (nanoDESI),[94] liquid extraction surface analysis (LESA),[95] liquid microjunction-surface sampling probe (LMJ-SSP),[96] probe electrospray ionization (PESI)[97] and others.[7,8] On the other hand, the laser-assisted desorption methods applied in IMS include laser ablation electrospray ionization (LAESI),[98] laser electrospray mass spectrometry (LEMS),[99] electrospray laser desorption ionization (ELDI),[100] atmospheric pressure-MALDI (AP-MALDI) and others.[7] Here, we mainly highlight the DESI and LAESI, as examples of a solid–liquid extraction method and laser-assisted desorption, and then expand their basic principles to other related techniques, as well as AP-MALDI, that are also applied in IMS.

Desorption Electrospray Ionization

DESI has been utilized for more 10 years and is one of the most established ambient ionization methods applied in academia, medicine, and industry.[101] Going further than IMS, similar to MALDI-IMS, DESI scans samples continuously across targeted spots to compose one-dimensional (1D) linear profiling or two-dimensional (2D) spatial distribution of molecules. The typical spatial resolution of DESI-IMS is about one to a few hundreds micrometers, and 35 μm spatial resolution has been achieved, depending on the operation factors.[102] DESI-IMS has been improved greatly over the past 10 years, but there are still some drawbacks that also exist in other solid–liquid extraction ionization methods, for example, ionization efficiency and imaging spatial resolution, that need to be strengthened. The ionization efficiency of DESI depends on sample surface, electrospray parameters, chemical parameters, and geometric parameters (Figure 2(a)). Surface effects include chemical composition, temperature, and electric potential applied. Electrospray parameters include electrospray voltage, nebulizing gas, and liquid flow rates. Chemical parameters refer to the sprayed solvent composition. Geometric parameters include incident angle, collection angle, sprayer tip to sample surface distance, and MS inlet to surface distance. The aforementioned parameters further affect imaging spatial resolution. In the next section, we detail sample preparation, solvent decision, limitations, and improvements to DESI. Then some other solid–liquid extraction techniques are introduced.

Sample Preparation and Solvent Decision

DESI and other ambient ionization techniques share the obvious advantage of which almost no sample preparation is required. But for nonflat, soft, fluid, or irregular samples, proper sample preparation may still be necessary. Sections or cryosections of plant seeds, flowers, and stems can be prepared for IMS to reveal the molecular distribution inside the organs.[103,104] However, the surfaces of leaves and flowers are not always flat thus limiting the collection of high-quality IMS data. An alternative method is to

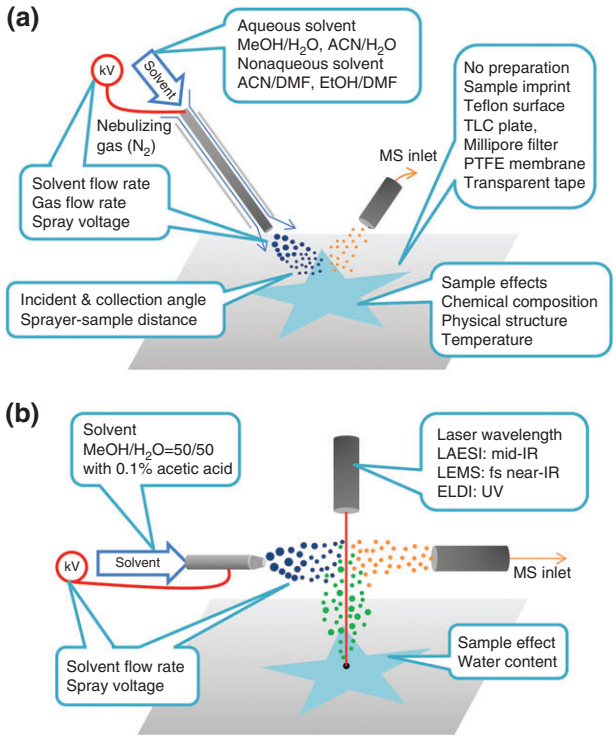

FIGURE 2 | Schematic overview of ambient ionization mass spectrometry. (a) The concept and improvement of desorption electrospray ionization (DESI) and its parameters: sample effects, electrospray parameters, chemical parameters, and geometric parameters. (b) The concept and improvement of laser ablation electrospray ionization (LAESI) and its parameters: sample effects, electrospray parameters, and chemical parameters.

imprint the uneven samples onto another flat absorbent surface. A Teflon surface can absorb the analytes from different plant materials and improve the spatial resolution and sensitivity of IMS analysis compared with the results acquired from direct scanning analysis.[103,105–107] DESI-IMS can also be used to readout thin-layer chromatography (TLC) plates. With some proper chemical or physical treatment, MS signals of the fruit, leaf, seed, and root sections blotted on TLC plates,[108,109] are enhanced. On the other hand, microbial colonies on agar are usually scanned directly if the agar and colonies are hard enough. Imprint techniques can also improve the quality of DESI-IMS for soft agar and fluid colonies. Imprinting *Bacillus* and *Streptomyces* onto the Millipore HA filter membrane,[110] *Streptomyces* onto a polytetrafluoroethylene (PTFE) membrane,[111] and *Fusarium* onto TLC[8] are examples of how DESI-IMS quality has been enhanced with irregular, soft samples. Three fungi, *Pythium*, *Trichoderma*, and *Moniliophthora* cultured on potato dextrose agar (PDA) can even be imprinted conveniently and fast using commercial transparent tape.[112,113] Recently, electrospun nylon-6 nanofiber mats have also been applied to imprint healthy plant organs and fungal-infected fruits for DESI-IMS analysis.[114] Some other imprinting materials are not only utilized for DESI-IMS but also for SALDI-IMS, although those materials do not provide a universal improvement in detection for all analytes.

Solvent composition is the main factor for solid-'liquid' extraction ionization as it determines what and how many analytes can be detected. The microextraction and charge transfer efficiency between charged droplets and analytes relies heavily on solvent composition.[7] Spray solvent composition and choice usually follows the reported extraction methods of target analytes. For most tissue (plant and animal) section samples, methanol/water and acetonitrile (ACN)/water are used, but such solvent compositions have also been determined to be harmful and destructive methods to some animal sectioning samples.[115] Although methanol/water is most widely applied in DESI-IMS, other solvent compositions have been proposed to utilize and improve the data quality. For example, ACN with dimethylformamide (DMF) and ethanol with DMF are two nonaqueous, biological sample-friendly solvent mixtures that enhance the lipid signal intensity and imaging quality without damaging the sample, which can be used in further experiments.[116] Additionally, chloroform/ACN/water has been utilized in DESI of leaves and petals for detecting the very long-chain fatty acids.[117]

Instrument Derivation, Improvements, and Strategies

Other solid–liquid extraction methods are similar to DESI but they use different mechanical structures. The obvious difference is that although LESA, LMJ-SSP, and nanoDESI have solvent sprayers that are very close to the sample surface, DESI has a solvent sprayer that is more separated from the surface.[8] Only three ambient solid–liquid extraction methods applied in IMS have been commercialized, DESI, LESA, and LMJ-SSP. NanoDESI is a homemade machine whose concept is derived from DESI.[118]

LESA is based on generating a submillimeter solvent droplet (ACN, methanol, 0.1% formic acid, and so on) by pipette tip dropping on the sample and mechanically transferring the tip containing the extract into the inlet of ESI or nano-ESI.[119] The solvent droplet is a crucial factor for spatial resolution of LESA-IMS. LMJ-SSP also uses a similar concept to LESA but LMJ-SSP can extract the sample continuously. LMJ-SSP utilizes a coaxial tube that contains inner and outer capillaries. The solvent flows from the outer capillary approaching the sample surface

for microextraction. The soluble analytes dissolve in the liquid droplet and are consequently transferred along with the liquid flow to the ionization source through the inner capillary.[96] The distance from acme of the coaxial tube to the sample surface is a critical factor that influences the spatial resolution. The general spatial resolutions of both LESA and LMJ-SSP are around 1000 μm which is larger than the general level experiments of DESI-IMS and MALDI-IMS.[95,96] Hence, LESA and LMJ-SSP are sometimes used to assist other high spatial resolution IMS techniques in the detection of small molecules.[32]

NanoDESI can overcome some of the disadvantages of DESI. The basic structure of nanoDESI is two capillaries with one of their end tips close to each other so as to create a liquid bridge on the sample surface. The solvent flows continuously from primary capillary onto the sample surface and the extract is drawn into the nanospray capillary then transferred to the MS inlet immediately.[118] The nanospray scale (50 μm inner diameter) tips of capillaries can form a micrometer scale of liquid bridge on the surface. Therefore, nanoDESI-IMS can raise the spatial resolution (100 μm, typically; ~10 μm, the best) similar to DESI.[94] In addition, the morphology of the sample, such as a tissue section, can be kept almost intact because the solvent flows lightly over the surface.[120]

Overall, DESI and other solid–liquid extraction methods are still being invented and improved. Easy ambient sonic-spray ionization (EASI),[121] PESI, and scanning probe electrospray ionization (SPESI)[122] are such examples. The critical factor, spatial resolution, is strongly related to the size of the solvent sprayer and the distance between the sprayer and the sample. The amount of solvent and the composition significantly affect the sensitivity. However, there is a trade-off between sensitivity and spatial resolution in IMS, which is determined depending on the purpose. Sensitivity is negatively correlated to spatial resolution, so plenty of solvent compositions are recommended to scan an unfamiliar sample. When the molecules are targeted, strengthening the spatial resolution of IMS is most suitable.

Laser Ablation Electrospray Ionization

LAESI was invented in 2007 and is still the only commercialized ambient laser-assisted desorption method.[98] LAESI combines 'laser ablation' with 'electrospray ionization' without matrix under atmospheric pressure (Figure 2(b)). Mid-infrared laser, for example, Er:YAG laser (2940 nm), is implemented in LAESI to activate the OH bond vibration of water in the sample. High-energy water gas particles are generated upon laser excitation and simultaneously ablate the analyte particles to the air. The gas phase particles are then ionized with charged droplets from the secondary ESI before entering the MS inlet.[98] The spatial resolution of LAESI-IMS is 200–500 μm depending on the size of the laser beam.[123] Similar to traditional ESI which can generate multiply charged ions, the mass range of detection of LAESI can extend from small molecules to biomolecules (proteins) of more than 66 kDa.[98]

Instrument Derivation, Improvements, and Strategies

The significant limitation of LAESI is that target samples need rich water content because ablation relies on water vibration. In addition, the ablated sites of the sample are irreversible for additional experiments.[98,123] This requirement is an obstacle for the use of LAESI on dehydrated tissue sections. In contrast, no pretreatment samples are suitable for LAESI-IMS because of the limited operating time and material. Hence, for instance, fresh plant tissue is efficiently ablated by a mid-infrared laser because of the high water content,[98,123,124] thus plant tissue is a good choice for LAESI-IMS.

The other two techniques, ELDI and LEMS are very similar to LAESI but with different laser pulse duration and wavelengths.[99,100] LEMS, as known as atmospheric pressure femtosecond laser imaging mass spectrometry (AP fs-LDI IMS), uses a near-infrared femtosecond laser (800 nm) beam to ablate the sample surface.[99] The analyte desorption is through a nonresonant energy supplied by a high-density laser with a 20-μm diameter laser beam spot. However, as a large amount of fragmentations are generated during excitation, the obvious disadvantage of LEMS is the limitation of the mass range of detection, which can be no more than *m/z* 400. ELDI utilizes a 337-nm UV pulse nitrogen laser beam to construct the IMS with 200 μm resolution.[125] Similarly, ELDI does not need any sample pretreatment or matrix; nonetheless, an iron (II, III) oxide (Fe_3O_4) coating must be applied on the sample if the target compound is over *m/z* 800 to 1200.[126]

For general IMS users, LAESI would be primary choice of matrix-free ambient laser-assisted desorption method. Although the water content is the obvious limiting factor, high water content and irregular samples like plant tissue are not a problem. Moreover, thin animal tissue cryosections still can be scanned by keeping water in the tissue section and preserving the sections at low temperature.[127] Ambient laser-assisted desorption methods are still not a

popular IMS technique and most methods are in the optimization stage. How to expand the field of application such as in plant biology, and strengthen the imaging quality and sensitivity would be priorities to achieve wide commercialization of the ambient laser-assisted desorption method.

Atmospheric Pressure-MALDI

AP-MALDI, based on the principle of MALDI has been commercialized. It conveys several components as well as advantages and disadvantages of MALDI-MS. Sample preparation and matrix deposition are followed by conventional vacuum MALDI-IMS and the laser ion sources and mass analyzers in MALDI-MS can be incorporated with the AP-MALDI MS. One benefit of AP-MALDI-MS is less fragmentation of analytes, which may influence the detection of targets, and is due to the collisional cooling of the analytes with neutral gases.[128,129] Moreover, some of analytes or matrices are much more stable under the ambient condition in comparison with the high vacuum condition. However, the efficiency of transferring the ions from samples to the analyzers still needs to be improved, such as by utilizing field-free transmission with geometry matrix.[130] The spatial resolution of AP-MALDI-IMS also mainly depends on the laser spot size, which is about 5–7 μm and can even be utilized on compositions at the single-cell level.[131] And it can also be applied on several biological samples, including animal tissues[130,132] and plant tissues,[133] although most of studies still focus on 1D linear profiles not 2D distribution.

METABOLITE IDENTIFICATION AND QUANTIFICATION

Combining with High-Resolution Mass Analyzers

The crucial factor in IMS is resolution, including spectral and imaging resolution. Use of a high-resolution analyzer can provide accurate molecular weight. Fourier transform ion cyclotron resonance (FTICR) and orbitrap provide the highest spectral resolution. The analyzer with the second highest resolving power is TOF, with ion trap (IT) and quadrupole analyzers considered to be the third tier. Although TOF, IT, and quadrupole analyzers cannot offer extremely high spectral resolution, they can still assist FTICR and orbitrap with their efficient acquisition speed to scan an abundance of small molecules. For MALDI-IMS, TOF and TOF/TOF are common, cheaper, and faster analyzers for both macro and small molecules. However, FTICR and orbitrap combined with a MALDI source are more efficient due to their high resolution and not having a limitation on small molecules. Orbitrap combined with IT and quadrupole or FTICR itself can collect the tandem mass data, enhancing molecular identification. With respect to ambient ionization, triple quadrupole, quadrupole-TOF, IT, FTICR, orbitrap, and other hybrid analyzers are also utilized to present high-quality resolution.

For some molecules with the same molecular weight but different structures, ion mobility spectrometry can strengthen the molecular separation ability after the ionization and before the detector. The ion mobility system contains the buffer gas in the drift tube which is used to separate the ionized molecules based not only on the mass, but also on charge, size, and shape of molecules. For example, analyzing ribosomal or nonribosomal peptides, oligonucleotides and lipids by ion mobility spectrometry gives a chance to differentiate many kinds of isomeric type. Ion mobility spectrometry can be used together with MALDI and an ambient ionization source IMS system. The former was utilized on animal tissues for detecting various lipids,[134] and the latter, for example LAESI, was used to differentiate isobaric ions from the plant leaf sample.[135] In short, ion mobility spectrometry provides a new dimension—drift time incorporating to the *m/z*, intensity, and spatial information in IMS.

Metabolite Identification

High-resolution MS and tandem MS data can offer accurate molecular weight together with fragment information about a molecule, which contribute to successful metabolic identification/dereplication. Several databases and tools allow users to analyze MS and tandem MS data intuitively and systematically. IMS can only collect MS and tandem MS *in situ*; therefore, it is unable to provide an efficient separation of analytes like LC-MS to enhance detection of molecular diversity. Hence, LC-MS and LC-MS/MS are commonly applied in metabolomics research to assist the identification of target molecules revealed in IMS analysis (Figure 3). Although most IMS techniques have a limitation in the collection of sufficient tandem MS data such as LC-MS, MALDI, and DESI-IMS are still capable of utilizing selected reaction monitoring to reveal the distribution of known molecules whose fragments would be better targets to be localized. For targeting rifampicin and some lipids in tissue sections, high-resolution MALDI MS/MS-IMS data not only aided

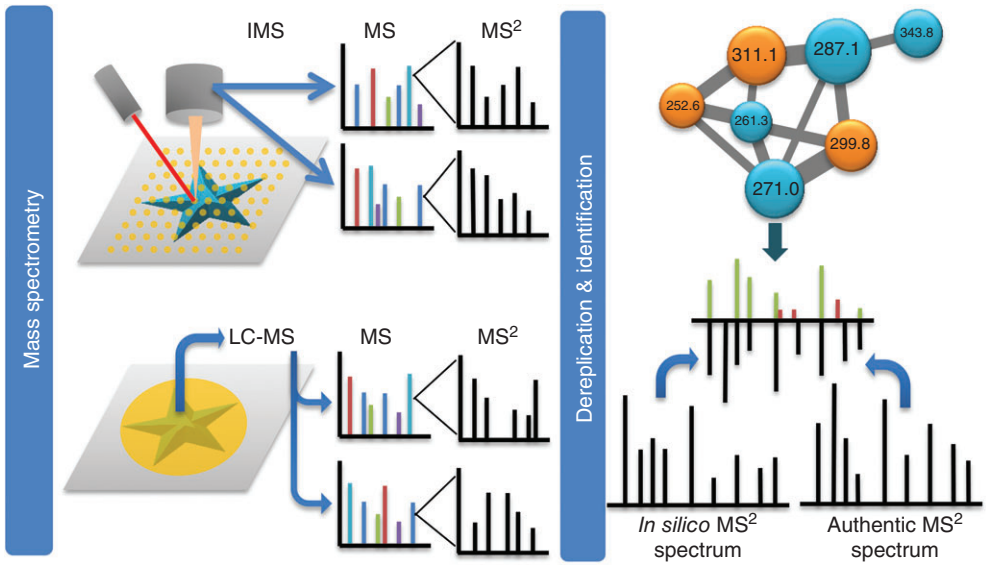

FIGURE 3 | Workflow of imaging mass spectrometry (IMS) coupled with liquid chromatography-mass spectrometry (LC-MS)/mass spectrometry (MS) for metabolomics. IMS offers a MS spectrum at every single location and LC-MS/MS supports IMS with overall metabolite information of targets. MS and MS^2 data are compared, dereplicated, and identified by networking tools and both authentic and in silico spectral databases.

compound identification but also increased sensitivity of analytes especially in a complicated sample matrix when detecting the fragments of specific analytes.[136] High-resolution DESI-IMS, applied to a bacteria–bacteria interaction study, directly identified multiple important secondary metabolites secreted by *Bacillus*, *Streptomyces*, and so on through MS/MS and molecular networking analysis.[137]

Many tools and databases have been constructed to deal with mass spectra.[138] For instance, Global Natural Products Social Molecular Networking (GNPS) is a tool and database using a molecular networking system to clarify groups of molecules depending on molecular weight and MS/MS spectra.[137,139] The GNPS presents results in a visually and similar MS/MS fragmentation patterns are clustered together. Using this elucidation and dereplication method, GNPS can deal with a lot of MS/MS data. The *In Silico* MS/MS DataBase (ISDB) is a database of predicted MS/MS spectra of natural products that can be used in conjunction with GNPS to support identification and annotation of individual MS/MS spectra.[140] The predicted MS/MS database of ISDB was generated from the commercial dictionary of natural products (DNP) recording comprehensive natural product structures. CSI:FingerID is another tool for dereplicating unknown tandem MS spectra with the small molecule databases like PubChem.[141] Like ISDB, CSI:FingerID can compare tandem MS data with the predicted fragments (fingerprints) of molecules and give them a matching score objectively. On the other hand, isotope patterns offer important information to predict molecular formulas from high-resolution mass spectra. Sum formula identification by ranking isotope patterns using mass spectrometry (SIRIUS) is one of the tools that combine MS isotope patterns and tandem MS fragmentation to identify metabolites.[142] ReSpect is a MS library used mainly for identifying plant metabolites and it has an abundance of tandem MS spectra collected from the literature for plant metabolomics research.[143] MassBank also contains authentic small-molecule tandem MS spectra with different ionization and collision-induced dissociation factors.[144] The Human Metabolome Database (HMDB) is a good choice for freely searching small molecules in humans through MS and tandem MS even connecting to 1D and 2D NMR data.[145] The Metlin metabolomics database has the most true high-resolution MS/MS spectra of metabolites and resources that mainly come from human metabolites. Also its MS/MS data includes different ionization methods, collision energies, and high-resolution analyzers.[146] In addition, various 'niche' databases have also been generated. For instance, Antibase and AntiMarin are specific for microbial and marine natural products, and can connect to NMR and other spectroscopic data. MarinLit is a database supporting marine natural product identification. LipidBlast is a specific powerful *in silico* tandem MS database for lipid identification.[147]

Additionally, we can also mine some information about small metabolites through whole genome analysis. For example, 'antiSMASH' allows genome searches to find out and annotate the secondary metabolite biosynthesis gene clusters from microorganisms.[148] It helps to find the potential predicted metabolites and identify the known metabolites derived from specific gene clusters. Moreover, 'Pep2Path' is a genome mining tool that explores all similar gene clusters that could biosynthesize the ribosomal and nonribosomal peptides predicted based on tandem MS fragmentation.[149] The Genome-to-Natural Products platform is another integrated database, based on genome and LC-MS/MS data, which is a platform mainly for polyketide and nonribosomal peptide identification.[150] In summary, identification and dereplication using these databases and tools are common and usual steps in IMS and LC-MS analysis.

Quantification

The localization of metabolites on sample surfaces has been successfully analyzed by various IMS techniques. However, a problem with these IMS techniques is that measurements are usually made on a qualitative basis. Accurate quantification is essential for multiple sample analysis. Although LC-MS supplies absolute quantitation, spatial information of small metabolites within samples are lost during the sample homogenization. Quantitative whole body autoradiography (QWBA) enables the absolute quantification of examining molecules and provides the distribution of labeled molecules that do not distinguish between the labeled compounds and their derived metabolites. In recent years, quantitative IMS (QIMS) was developed as a complementary technique to classical analytical techniques, such as LC-MS and QWBA. However, the limitation of QIMS is that the signals are affected by many factors such as the matrix effect, extraction efficiency, and ion suppression effects.[151]

Quantification strategies for MALDI-IMS have developed into on-tissue, under-tissue, in-tissue, and in-solution methods (Figure 4(a)). The in-solution method deposits the standard onto the target sample plate giving the calibration range. However, the matrix effect and extraction efficiency cannot be established while using the in-solution method. For this reason, an internal standard is used for the calibration of the ion intensities and the compensation of the ion suppression effects.[152] QIMS can be achieved by spray-coating and microspotting an internal standard on, under, or in the tissue section,

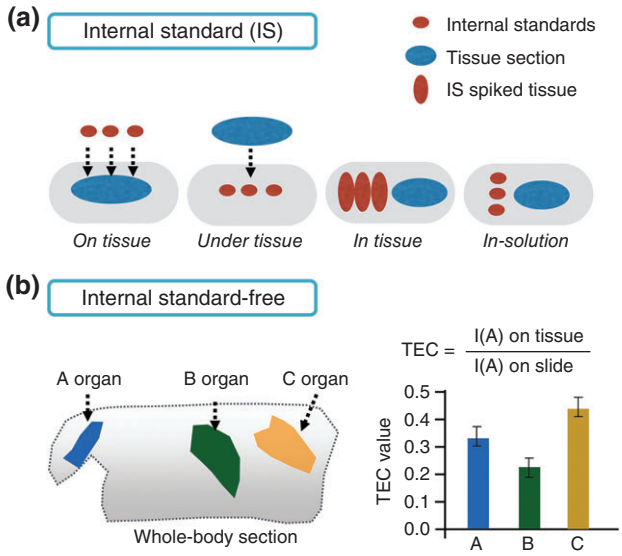

FIGURE 4 | Illustration of depositing internal standard (IS) methods and an IS-free method for quantitative imaging mass spectrometry (IMS). (a) Depositing IS on the tissue section requires mounting the section followed by application of the IS. Deposition under the tissue section requires spotting the IS first, and mounting the section on top. Deposition in the tissue section requires homogenized tissue samples and then the internal standard is incorporated in the tissue homogenates. Deposition in solution requires that standard solution is directly spotted on the sample plate. (b) Left, animal tissue sections and their matrix-assisted laser desorption/ionization (MALDI)-IMS. Right, tissue extinction calculation (TEC) values as histograms for each targeted organ.

preferably an isotopically labeled internal standard because such a standard has similar extraction and ionization efficiency to the target analytes.[153] Recently, Chumbley et al. compared the different internal standard application methods with LC-MS for quantitation.[154] The results showed that depositing the standards on the tissue came closer to the results achieved with the LC-MS approach. The on-tissue strategy was demonstrated with the quantification of glucosinolate on *A. thaliana* leaf surfaces by spotting glucosinolate standards.[155] Internal standards mixed with fluorescent dye were transferred on the leaf surface and covered with matrix by sublimation. This strategy was validated with other surface analysis methods, such as LAESI[156] and LESA-MS and showed a high correlation. However, internal standard-based QIMS is only suitable for a specific analyte and sample combination. Therefore, internal standard-free QIMS techniques, such as the use of tissue extinction coefficient (TEC) were developed (Figure 4(b)). TEC was used to calculate the ion suppression of a target molecule in a tissue region of interest.[157] Through this process, a strong correlation

between TEC quantitative data and reference data deduced from LC-MS has been demonstrated and the target molecules were then quantified in up to 25 different tissues at the same time without additional labeling.

For DESI QIMS, the internal standards can be applied in two different ways: (1) mixing the internal standard together with the spraying solvents[158] and (2) micropipetting the internal standard on the sample tissues.[159] Lanekoff et al. added isotopically labeled standard to the solvent to compensate for ion suppression and demonstrated the utility of nano-DESI imaging for the detection of nicotine in rat tissue sections.[158] Vismeh et al. used DESI-IMS for localization and quantification of clozapine in rat brain sections.[159] To avoid possible redistribution of clozapine, the internal standard was slowly micropipetted rather than sprayed on top of the clozapine-containing tissue. The results demonstrated that DESI QIMS by micropipetting the internal standard is in excellent agreement with the LC-MS quantification approach.

QIMS is still far from perfect and the applicability of these methods will need validation and application to numerous analytes and sample combinations in the future. Despite the fact that various QIMS techniques have been developed, data processing is time-consuming data analysis. Recently several data processing software packages including signal preprocessing, multivariate analysis have been developed to make QIMS accessible.[160,161] With appropriate sample preparation for the incorporation of internal standards and analytes, together with tissue-specific normalization, QIMS applications have potential for success. In this section, we have summarized some QIMS strategies and applications in Table 1.

MULTIMODAL IMAGING SYSTEMS

Each IMS technique has its own limitations and strengths. The combination of multimodal imaging systems has been demonstrated in plants, animal tissues, and microbial metabolite research.[165–167] For instance, IMS can be combined with magnetic resonance imaging (MRI)[168] to harvest more detailed structural and molecular information. Recently, not only the combination of IMS and other imaging techniques but also multimodal IMS systems have been developed to provide extra spatial information and/or a wider mass range, such as MALDI with SIMS[169] and MALDI and SALDI.[64] In this section, we summarize recent combinations of imaging systems that have been used to obtain additional morphological and structural, chemical information, and present selected examples. The comparison of various imaging techniques was showed in Table 2.

Fluorescence and Staining Techniques by Microscopy with IMS

Fluorescence imaging is a powerful and popular technique that can be divided into fluorescence staining imaging and a fluorescent protein labeling imaging system. Fluorescent protein labeling is another popular technique whereby a reporter gene encoding green fluorescent protein (GFP) or red fluorescent protein (RFP) is inserted into the promoter region of a gene

TABLE 1 | Overview of Different Quantification Approaches of Various Imaging Mass Spectrometry (IMS) Techniques

	Internal Standard (IS) Preparation	Analyte/Sample Type	Calibration Range	References
Matrix-assisted laser desorption/ionization (MALDI)	IS deposited under tissue	Cocaine/animal tissue section	0.03–0.5 ng	162
	IS microspotted on tissue	Tiotropium/animal tissue section	0.08–2.6 pmol	163
	IS microspotted on tissue	Glucosinolate/plant tissue	0.976–500 pmol	155
	IS spiked within homogenate of animal organ	Lapatinib and nevirapine/ animal tissue section	62–61,600 ng/g	164
	Analytes spotted on the slide (in solution)	Propranolol and olanzapine/ whole body sections of mice	0.02–10 pmol for Propranolol; 1–60 pmol for olanzapine	157
Desorption electrospray ionization (DESI)	IS mixed with the spraying solvents	Nicotine / animal tissue section	1.6–10.5 uM	158
	IS micropipetted on tissue	Clozapine/animal tissue section	0.1–100 ng	159

TABLE 2 | Comparison of Various Imaging Techniques

	Raman Imaging	Fluorescence Imaging	Magnetic Resonance Imaging (MRI)	Imaging Mass Spectrometry (IMS)
Chemical information	Functional groups of biomolecules	Fluorescence or biomolecules with fluorescent labels	Abundance of hydrogen atoms	Molecular weight and fragmentation of biomolecules
Analyte specificity	Low	Moderate to high	Low	High
Analyte diversity	High	Limited	Low	High
Morphological information	NA	Yes	Yes	NA
Spatial resolution	nm–μm[170]	nm[171]	nm–μm[172]	nm (SIMS)–μm (MALDI, DESI)
Sample type	Noninvasive, live cells	Noninvasive, live cells	Noninvasive	Fresh sample (AIMS), dehydrated sample (VIMS)
Sensitivity	pM (SERS)[173]–mM (Raman Spectroscopy)[174]	~fmol	μM–mM	pM–mM
Acquisition time	~seconds/sample point (Typical Raman microscopy)[170], ~milisecond/pixel (coherent Raman imaging)[175]	milisecond–minutes[171]	milisecond (Real-Time MRI)[176]–minutes	~milisecond/pixel (MALDI-TOF)[61]–seconds/sample point (DESI)

NA, not available; AIMS, ambient IMS; VIMS, vacuum IMS.

of interest. This approach allows real-time monitoring of gene expression within a living cell as a molecular reporter tool that enables the clarification of biological processes and pathways. The tandem dimer Tomato (tdTomato) is a member of a family of fluorescent proteins used as genetically encoded fusion tags in an animal model and cell cultures[177] to visualize hypoxic tumor regions.[178] The IMS of tdTomato was used in the research of breast tumor xenografts.[179] The distribution of a tdTomato tryptic-peptide (*m/z* 2225.0) was mapped in the hypoxic regions by IMS. The localization analysis of the tdTomato deduced from IMS and fluorescence microscopy resulted in a relatively high correlation. With this approach, it is possible to map the biomolecules that are up or down regulated in hypoxic tumor regions to understand hypoxia-induced changes in cancer. Fluorescence imaging was also used to monitor matrix-producing cell subpopulations of *Bacillus subtilis* biofilms.[180] Si et al. applied MALDI-IMS to study cellular differentiation and molecular heterogeneity in *B. subtilis* biofilms. Fluorescence imaging data showed the distribution of matrix-producing cell subpopulations. To correlate fluorescence imaging data with IMS information, the differences in biofilm signaling, cannibalistic factor distribution, and matrix-related gene expression were observed (Figure 5(f)). These two complementary imaging approaches provide new insights into cannibalism in biofilm development.

For fluorescence staining imaging, 4′,6-Diamidino-2-phenylindole (DAPI) is a fluorescent stain capable of passing through the intact cell membrane and binding to an A-T region of DNA. Therefore, it is very useful for staining living cells. In some studies, Ong et al. used a combination of IMS and DAPI fluorescence imaging to differentiate peptide dynamics in *Schmidtea mediterranea* during cephalic ganglia regeneration.[181] Insights into the peptides associated with cephalic ganglia regeneration in *S. mediterranea* could be achieved with IMS. The ganglia were clearly visible in 12-day regenerated planarians but not at the early stage with the IMS map. However, a cephalic ganglia-like structure was visualized in 6-day regenerated planarians by fluorescence staining imaging. Using the fluorescence staining imaging data as a guide, the IMS data for 6-day regenerated planarians were recollected and showed a weak ion signal of *m/z* 1907.3. This demonstrates fluorescence staining imaging is able to validate IMS results as a complementary imaging technique. On the other hand, with the fluorescence *in situ* hybridization (FISH) technique, a fluorescently labeled probe is used to bind a specific DNA or RNA sequence from biological samples. This makes it possible to correlate the metabolic production with taxonomic identification such as in environmental microbial samples by the combination of IMS and FISH. Kaltenpoth et al. used this approach to reveal similar distribution of the cell population and various symbiont-

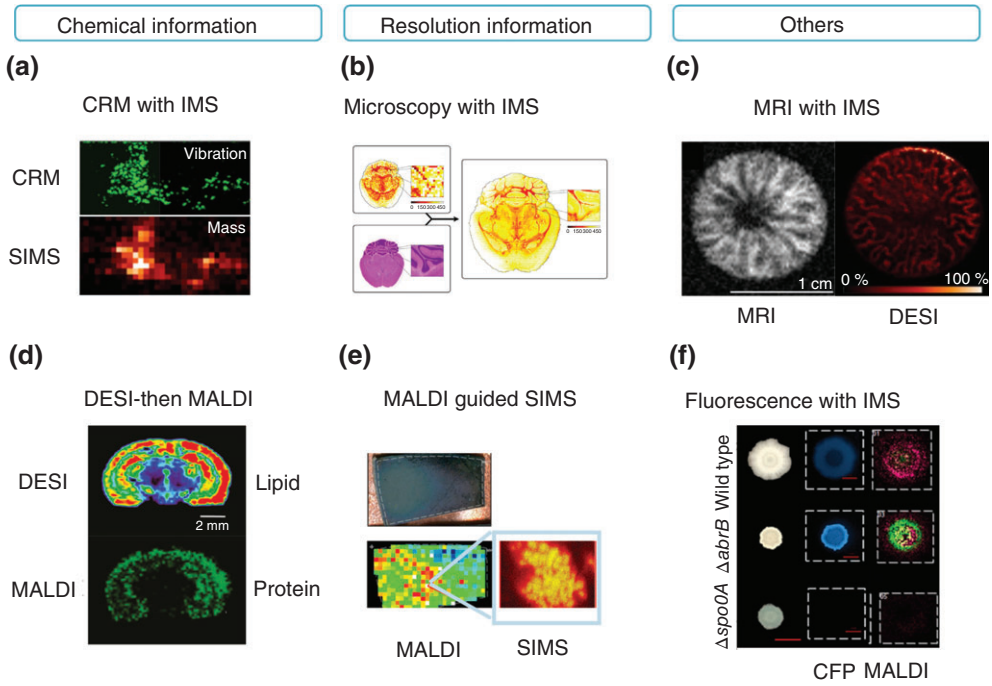

FIGURE 5 | Selected examples of multimodal imaging mass spectrometry. (a) Confocal Raman microscopy (CRM) and secondary ion mass spectrometry (SIMS) imaging MS of quinolone molecules in Pseudomonas-derived biofilms. (b) Microscopy and matrix-assisted laser desorption ionization (MALDI) imaging mass spectrometry (MS) of lipids in mouse brain. (c) Magnetic resonance imaging (MRI) and desorption electrospray ionization (DESI) imaging MS of protonated arecoline in in areca nut.(d) DESI then MALDI-IMS for lipid and protein distribution in mouse brain tissue. (e) MALDI-guided SIMS for imaging of metabolites in bacterial biofilms. (f) Fluorescence imaging and MALDI-IMS in Bacillus subtilis biofilms. The chemical information column presents additional chemical information by multimodal combination. The resolution information column presents additional resolution information by multimodal combination. Other columns present additional morphological, and gene expression information by multimodal combination. (Reprinted with permission from Refs 188. Copyright 2010 American Chemical Society (a), 183. Copyright 2015 Nature Publishing Group (b), 185. Copyright 2016 Elsevier Ltd. (c), 166. Copyright 2012 Elsevier Inc. (d), 192. Copyright 2014 American Chemical Society (e), and 180. Copyright 2016 American Chemical Society (f))

produced antibiotics in the defensive symbiosis between *Streptomyces philanthi* and beewolf wasps.[182] This combination can detect a broad range of small molecules for studying microbial interactions *in situ* and linking metabolic profiling to gene expression.

In addition, a combination of IMS and histological stains by microscopy allows the acquisition of information about molecular distribution at high spatial resolution together with abundant morphological information. This combination is commonly applied in histological studies of animal tissues, human, and clinical samples. The challenge of the microscopy/IMS combination, especially for histological staining samples, is how to avoid damage during the IMS process. In DESI-IMS, a spray solvent of *N*, *N*-dimethylformamide with water or methanol is considered to be a morphologically friendly solvent system that does not damage tissue slices after DESI probe scanning.[115] For MALDI-IMS, histological stains are used after removing the matrix by rinsing the tissue samples with ethanol.[116] Another solution is to predict molecular distribution in a non-IMS measured tissue by sharpening molecular distribution.[183] This method succeeds in predicting the distribution of lipids in tissue sections at 10 μm resolution (reconstruction score: 82%) from the images of 10 μm microscopy and 100 μm IMS (Figure 5(b)). The advantage of an image sharpening application is that it can overcome the physical limits of IMS techniques (such as laser beam size) by combination with high spatial resolution microscopy imaging. However, the measured ion images can only be predicted with a high reconstruction score. Analytes with low reconstruction score (weak relationships) can also be found, but they are not recommended for use in microscopy imaging and fusion prediction. Immunohistochemistry (IHC) could be coupled with MALDI-IMS to investigate tumor and animal tissue sections. The combination of IHC and IMS enables monitoring the efficacy of cytotoxic antibody treatments as a novel clinical

application.[184] However, IHC has mainly been used to reveal the presence of specific antigens (proteins) rather than small molecular compounds. In the future, this technique might be used to expose the specific abnormal regions for correlating with small molecule distribution in IMS studies.

MRI with IMS

MRI, a medical imaging technique uses strong magnetic fields, field gradients, and radio waves to generate images of the inside of the target samples. MRI enables a three-dimensional (3D) anatomic structure of a sample of interest with significant resolution and gives a precise sample shape in a noninvasive manner. Combining IMS techniques with such a detailed structural representation can be useful. The combination of MRI and IMS has been used for monitoring the inflammatory response in mice infected by *Staphylococcus aureus*.[137] However, to date, few reports have demonstrated the analysis of small molecule distribution by using MRI and IMS. Srimany et al. used MRI and DESI-IMS to study the associated change in the alkaloid content during the growth of a nut[185] (Figure 5(c)). The commercial PAXgene fixation pipeline was applied prior to MRI for 3D MALDI-IMS.[186] Oetjen et al. applied the experimental and computational workflow pipeline for MRI-compatible 3D MALDI imaging mass spectrometry. This multimodal image approach shows the feasibility of combining 3D MALDI-IMS with MRI to allow the correlation of molecular distribution with anatomic information. In addition, MRI has been demonstrated to quantify liver iron content.[187] Therefore, the combination of MRI and IMS might provide an opportunity for the correlation between the quantification of iron and related metabolites in target organs.

Confocal Raman Microscopy and Spectroscopy with IMS

Raman spectroscopy is a spectroscopic technique used to observe rotational and vibrational information in a system. It is a common biochemical analysis technique that provides a molecular fingerprint of identified compounds. Confocal Raman microscopy (CRM) is considered to be a high-resolution and noninvasive imaging technique that yields information about functional groups as a function of location. The combination of CRM and SIMS-IMS has been used for understanding detailed chemical and structural information during pre-enzymatic processing of lignocellulosic materials (LCMs)[188] (Figure 5(a)). LCMs consisting principally of cellulose, hemicelluloses, and lignin have attracted interest because of their potential for biofuel production.[189] Through this approach, the assignment of intracellular globular structures to hemicellulose-rich lignin complexes was confirmed by correlating MS data and vibrational Raman scattering data from specific spatial positions. The combination of CRM and SIMS-IMS was used to visualize metabolites such as quinolone distribution in *Pseudomonas aeruginosa* biofilms.[190] CRM nondestructively detected broad molecules including carbohydrates, proteins, and quinolone-derived molecules. After CRM scanning, SIMS was performed at the same location and provided complementary chemical information to resolve ambiguous multiple quinolone metabolites which differ slightly in molecular weight. The combination of CRM and LDI-IMS was applied to understand the transfer of phytoalexins between banana plants and nematodes.[191] Hölscher et al. used LDI IMS to expose the distribution of anigorufone, a plant secondary metabolite on the lesions of root and individual nematodes. LDI-IMS showed that anigorufone was ingested and stored in the nematode body. Because anigorufone is nonwater soluble, it converges with lipids after being ingested; however, LDI-MS is incapable of detecting the non-UV absorbing molecules, such as lipids, so the authors used CRM to reveal the lipid distribution of yellow droplets and to correlate with LDI-IMS to demonstrate evidence of the anigorufone storage after ingestion. The aforementioned examples suggest that CRM not only provides high spatial resolution information but can also be used as a complementary tool to capture the molecules, which are undetectable by IMS.

Combination of Different IMS

The combination of various IMS techniques with different analytical capabilities might obtain additional molecular information and provide new insights. It is considered beneficial to harvest more information (about small to macromolecules) in the same tissue section or sample. For example, a single tissue can be first analyzed by DESI-IMS for lipid analysis with a histologically compatible solvent system, and sequentially analyzed using MALDI-IMS to collect peptide constituent information (Figure 5(d)). Finally, the tissue can be washed and stained with Hematoxylin and eosin (H&E) to reveal histological information.[116] In addition, MALDI-guided SIMS-IMS can achieve multiscale imaging of metabolites in bacterial biofilms (Figure 5(e)). Lanni et al. performed MALDI-IMS to obtain draft molecular distribution

of samples, which was used to direct subsequent SIMS-IMS to examine the molecules of interest from MALDI-IMS analysis.[192] Bioactive secondary metabolites rhamnolipids and quinolones from *P. aeruginosa* were detected and visualized on both the macro- and microscopic scales. This MALDI-guided SIMS-IMS approach has numerous advantages including specification of microscopic regions of interest from a chemical map, spatially registered micro- and macroscopic molecular images, and generation of a fiducial marker for sample navigation in SIMS-IMS. It can also be applied to other samples such as tissue sections where similar multiscale complexity exists. Phan et al. applied MALDI and SALDI for sample profiling and imaging the brain of *Drosophila*.[64] MALDI and SALDI approaches can provide complementary analysis of chemical composition. Although MALDI is suitable for analysis of a wide range of biomolecules, it is not easy to analyze small molecules (<*m/z* 600 Da) because of organic matrix interference, which can be overcome by SALDI-IMS. This combined IMS approach can provide the most diverse lipid images of the fly brain. Other multimodal IMS systems such as a commercial LMJ-SSP assisted MALDI-IMS have been applied to spatially reveal drug distributions in lung tissue sections.[193]

Multimodal imaging systems provide additional structural, chemical, morphological, and gene expression information. However, the feasibility of a multimodal imaging system is strongly related to sample preparation, which directly results in high or low quality of data. Optimizing sample preparation protocols together with improving the multimodal system interfaces for friendly operation and data analysis are crucial in this field.

APPLICATION OF IMS IN BIOLOGICAL INTERACTIONS

The critical advantage of IMS is the spatial distribution analysis at the molecular level, enabling it to offer crucial evidence of chemical variation of biological samples. Most cases are applications of IMS to animal organ sections, microbial colonies, and plant organ sections which present the inner molecular distribution and temporal change. However, IMS can be used to analyze more complicated systems, such as biological interactions. The study of the interaction between species is challenging because it is hard to separate each phase of the sample physically. In addition, utilizing molecular biology techniques is still restricted to the DNA, RNA, and protein levels, which rely on reporter gene systems revealing the position of a single or few targets. Most importantly, molecular biology techniques cannot directly detect small molecules. For these reasons, we can use IMS to 'see' the small molecules. IMS can be applied to directly detect molecules to show 'what' they are and 'where' they are in time. Furthermore, IMS can also help investigate multispecies and cross-kingdom systems such as plant-fungus or animal–bacteria interactions. Here, we highlight some studies mainly from 2014 that are important interaction cases. Also, we present some research directions that we believe are crucial but lack research using IMS; and targets that we believe are suitable to be tackled using an IMS-based strategy.

Microbe–Microbe Interactions

Microbes face keen competition in the environment, and use various strategies to fight for their environment niche. Antibiotics are one of the weapons they use against competitors. By applying IMS, we can directly observe compounds secreted by microbes to inhibit competitors. Furthermore, the secreted compounds may act as inducers or transmitters to others of the same species or cooperators. IMS can be used to elucidate the distribution of compounds and evaluate what the roles they play. Here, we highlight some examples of bacteria–bacteria, fungi–bacteria, and bacteria–other kingdom microbes.

Actinomycetes are group filamentous bacteria that produce abundant antibiotics and drugs and their interactions result in induction of secondary metabolites. *Streptomyces coelicolor* interacted with another five actinomycetes producing different kinds of metabolites[194] (Figure 6). *Bacillus* is also a predominant microbe that employs many antibiotics against competitors in the environment. *Bacillus cereus* secretes secondary metabolites which induce the biofilm formation of *B. subtilis*. Secreted diverse thiazolyl peptides were identified for employing MALDI-IMS and they also influenced other bacterial activities.[195] IMS is also an option in the search for antibiotics against human bacterial pathogens. The compounds from *Vibrio* sp. QWI-06 can inhibit human pathogenic *Acinetobacter baumannii*. Vitroprocines and other candidates secreted from QWI-06 were detected and their structures were elucidated using a LC-MS/MS assisted workflow and NMR.[196]

In the same way, bacterial metabolites that exhibit antifungal activity against plant–fungal pathogens can also be mined by IMS. Six *Lysobactor* species and strains isolated from soil, plants, and rhizospheres were found to have antifungal activity against

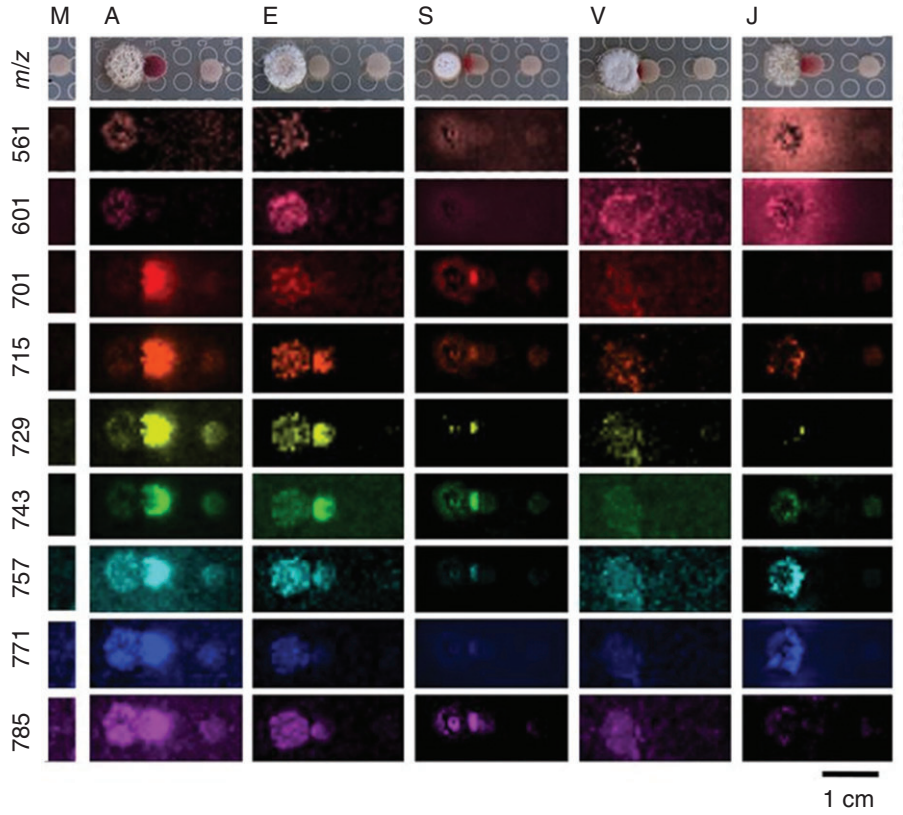

FIGURE 6 | Application of imaging mass spectrometry (IMS) to microbe-microbe interactions. IMS of Streptomyces–Streptomyces (or Amycolatopsis) interactions. Desferrioxamines B (m/z 561) and E(m/z 601) and acyl-desferrioxamines (m/z 701, 715, 729, 743, 757, 771, 785) are revealed by matrix-assisted laser desorption/ionization (MALDI)-IMS. M (S. coelicolor M145) represents only culture M145. A (Amycolatopsis sp. AA4), E (Streptomyces sp. E14), S (Streptomyces sp. SPB74), and V (S. viridochromogenes DSM 40736) represent the interaction with M145. Brightness indicates the intensity of the mass spectrometry (MS) signal. (Reprinted with permission from Ref 194. Copyright 2013 Traxler et al.)

soil-borne phytopathogen *Rhizoctonia solani*. At first, through genome mining, several secondary metabolite biosynthesis gene clusters were located in chromosomes such as terpene, siderophore, nonribosomal peptide synthase (NRPS), and polyketide synthase (PKS) gene clusters. Using this data, MALD-IMS was used to screen *Lysobactor* cocultured with *R. solani* and showed some small molecules and peptides signals on the area of inhibition zone.[197] These results present a good example of IMS-guided metabolomics combined with *in silico* genome analysis and *vice versa*. IMS also can assist screening the mutant lines with deficiency in antibiotic biosynthesis. Antifungal *Pseudomonas fluorescens* In5 and its derived mutant lines were cocultured with *R. solani* and *Pythium aphanidermatum*. The *P. fluorescens* In5 can inhibit two pathogens with nunamycin and nunapeptin, but other mutants present four kinds of phenotypes, and normally only inhibit one of the two pathogens or lose all antifungal activity. MALDI-IMS distinguished *P. fluorescens* In5 of none of the nunamycin or nunapeptin mutants and helped connect the antifungal genome clusters with metabolite data.[198]

Another surprising model is the interaction between bacterial phytopathogen *Ralstonia solanacearum* and soil fungus chlamydospore-formed *Aspergillus*. Chlamydospores are thick barrier spores that help the fungi survive in unfriendly temperatures and nutrient deficient conditions. *R. solanacearum* and some bacteria can trigger fungi to generate chlamydospores with secondary metabolites and the bacteria can hide in the spores to overcome a harsh environment. By employing MALDI-IMS, an LC MS/MS on *Aspergillus*, *R. solanacearum* GMI1000, and its *rmyA* mutant, ralsolamycin synthesized by PKS and NPRS hybrid gene clusters was confirmed to correlate with induction of chlamydospore formation and bacteria invasion.[199]

Protozoa are predators that hunt bacteria in the soil microbial ecosystem. In this kingdom, there are still many unknown species and relationships. Bacteria also have mechanisms to sense the attack of protozoa and defend against them. The relationship

between metabolites and the protozoa–bacteria interaction has been explored via MALDI-IMS and nano-DESI, and lipopeptides were found to be secreted by *P. fluorescens* SS101 that play crucial roles in inhibition of the encystment and recovery of the protozoa *Naegleria americana*.[200]

Plant–Microbe (Bacteria and Fungi) Interactions

Plants and microbes usually have two opposite relationships in ecosystem: parasitism and symbiosis. Fungi, bacteria, viruses, and nematodes are the four main pathogens that cause plant diseases. Fungal and bacterial diseases are responsible for a large proportion of the damage to crops (nematode and viral diseases are described later). The study of host/pathogen interactions is a key area for plant disease control. Nonetheless, molecular plant–microbe interactions research is mainly conducted using genomics, transcriptomics, and proteomics. Although application of the IMS method to plant pathology research is still not a mainstream technique, it has offered some unexpected output.

As an example of a plant–fungal pathogen interaction, multiple phytoalexins against grape downy mildew were induced after inoculation and observed by MALDI-IMS[201] and LDI-IMS.[202] Stilbene phytoalexins from grapevine can inhibit the growth of *Plasmopara viticola* zoospore.[203] Although not all stilbene phtyoalexins could be detected in these studies, the spatial distribution information may provide some insights about the interface of fungi and plants. In addition, MALDI-IMS data showed the distribution of two potential antimicrobial metabolites in pea leaves after *Fusarium solani* inoculation and also these two phytoalexins, pisatin, and pinoresinol monoglucoside were related to induction of *CHS* and *DRR206* genes in the pea leaf-infected sites[204] (Figure 7(b)). On the other hand, DESI-IMS supported by imprinting methods, detected important metabolites inside potato infected by *Pythium ultimum*, which is a severe soil-borne disease.[113] Through references to some potato metabolites pathways, several glycoalkaloids distributed at the infected sites were investigated using DESI-IMS.

Plant–bacteria are another area of particular interest in biotic stress research. The study of model plant *Arabidopsis* with MALDI-IMS could reveal the cross-species interactions. Epiphytic bacteria exist on the *Arabidopsis* leaf that can influence the leaf metabolome. Many insights about the interaction between the phytopathogen model strain *Pseudomonas syringae* pv. *tomato* DC3000 and *Arabidopsis* have been revealed by IMS techniques and have given new perspective to this relationship.[205] Utilizing MALDI-IMS imaging of *Arabidopsis*, various distributions of polysaccharides and amino acids were revealed that are related to nutrient and secondary metabolite biosynthesis after epiphytic bacteria and DC3000 inoculation. In addition, camalexin, a phytoalexin in *Arabidopsis*, was accumulated in leaves after DC3000 colonization, but not after epiphytic bacteria colonization.[205] IMS of crops also contributes to resistant breeding. Bacterial leaf blight of rice, caused by *Xanthomonas oryzae* pv. *oryzae* (Xoo), threatens rice yield all over the world. NALDI-IMS was successfully used to differentiate susceptible plants and plants resistant to Xoo[206] (Figure 7(a)). At the infection sites, the amount of general rice metabolites such as disaccharides, chlorophyll-a, phosphocholine, and monogalactosyldiacylglycerol were a little higher or showed no difference between susceptible and resistant lines. However, phytoalexins, momilactones, and phytocassanes, which were reported to be antimicrobial against Xoo, were revealed at the site of infection of the resistant rice. In contrast, two phytoalexins were not induced in the susceptible rice, which demonstrated that the obvious markers of the two lines are correlated with induction of phytoalexin biosynthesis gene clusters.[206] Another example of an endophytic pathogen, *Xylella fastidiosa*, which is bacterial pathogen exclusively colonized in citrus xylem. At the infection sites, hesperidin is related to the citrus defense mechanisms, and could be found by MALDI-IMS detection, which revealed a target applied on resistant inducer against *X. fastidiosa*.[207]

Small metabolites also participate in the complicated symbiotic relationship between plant hosts and microbes because members of the two kingdoms coordinate through those metabolites. The vital nitrogen fixation system, the association of *Rhizobium* species with legumes, is a well-known model of symbiosis. Using a combination of MALDI-IMS and LC-MS/MS, a powerful platform to clarify the secrets inside the legume nodule was created. A nodule composed of *Medicago truncatula* (plant) and *Sinorhizobium meliloti* (bacterium) is capable of nitrogen fixation; however, the nodule composed of *M. truncatula dnf1* and *S. meliloti fixJ* mutants is deficient in nitrogen fixation. Comparing the MALDI-IMS of these two nodules, 10 metabolites including some amino acids and derivatives were revealed inside the nitrogen fixation nodule.[208] Endophytic bacteria in plants sometimes produce extraordinary metabolites. Roots of *Putterlickia verrucosa* and *P. retrospinosa* contain the anticancer

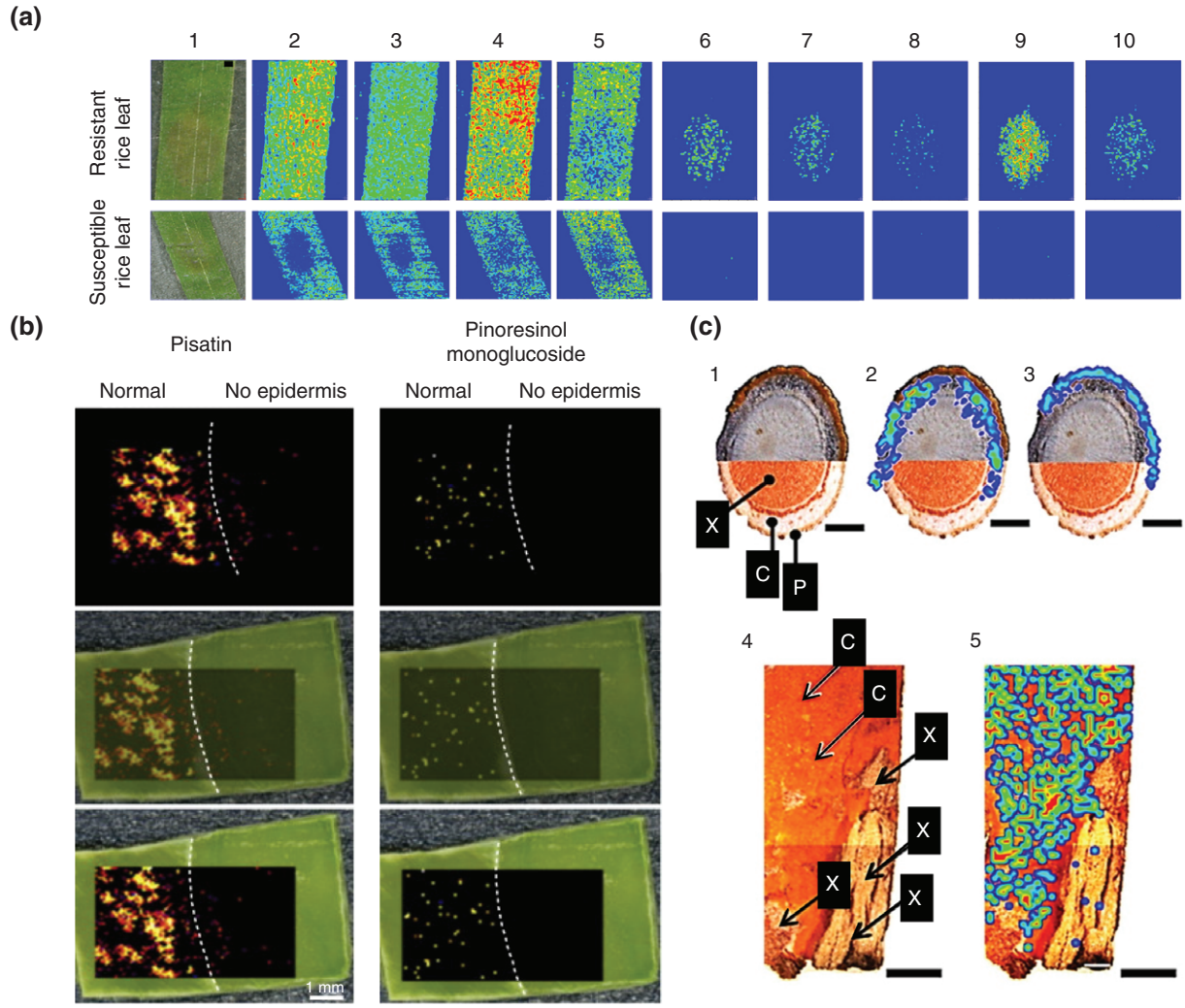

FIGURE 7 | Application of imaging mass spectrometry (IMS) to plant–microbe interactions. (a) IMS of rice resistant and susceptible lines leaves infected by Xoo. From Left to right: Optical image of the rice leaf with a black circle representing the inoculated region, phosphocholine (Pcho), disaccharide (sucrose), chlorophyll-a fragment, monogalactosyldiacylglycerol (MGDG), momilactone-A, momilactone-B, phytocassane-A, D, or E, phytocassane-B, and phytocassane-C. The intensity scales are represented as color-gradient relative intensities. (b) IMS of fungal pathogen inoculated pea pisatin and pinoresinol monoglucoside. The epidermal layer in the region of the right of the dotted line has been removed. Pisatin and pinoresinol monoglucoside presented in ratio of histology image layer (tissue image): IMS image data for image layer opacity at 100:100, 25:50, and 0:100 (from top to bottom). (c) IMS of maytansine in Putterlickia verrucosa root (X: xylem; C: cortex; P: periderm). 1. Transverse section of P. verrucosa primary root. 2. Distribution of maytansine in the cortex. 3. Distribution of phosphatidylcholine in the periderm. 4. Longitudinal section of P. verrucosa primary root. 5. Distribution of maytansine in the cortex. Black scale bars for panels 1–3 represent 500 μm and 4–5 represent 2000 μm. The intensity scales are represented as color-gradient relative intensities. (Reprinted with permission from Refs 206. Copyright 2015 American Chemical Society. (a), 204. Copyright 2015 Elsevier Ltd. (b), and 209. Copyright 2014 The American Chemical Society and American Society of Pharmacognosy (c))

metabolite, maytansine, which was produced by an endophytic *Actinosynnema pretiosum* containing AHBA synthase genes[209] (Figure 7(c)). Applying MALDI-IMS to scan plant root sections, maytansine was found mainly localized in the cortex but not in the periderm or xylem tissues. In addition, the plant growth promoting rhizobacteria (PGPR) colonizing on the root can also provide antibiotics or resistant inducers for the plant host. PGPR *Bacillus amyloliquefaciens* secreted surfactins outside tomato and *Arabidopsis* roots which was detected by MALDI-IMS. Moreover, MALDI-IMS also revealed surfactin diffusion over time, which is a great example of the application of IMS in time course assays.[210]

Plant–Insect Interactions

Herbivorous insects cause enormous crop yield loss. Plant–insect interaction is still usually explored

using GC- and LC-MS/MS-based metabolomics approaches. IMS can not only be applied on wounded plant reactions, but also utilized in herbivore insect physiology research after ingesting the crop; however, this approach is still rarely used. Soybean aphids threaten soybean plants worldwide and aphids influence changes in plant host metabolomes including changes in phytohormones as revealed through a soybean transcriptome study.[211] MALDI-IMS demonstrated that many phosphocholine and amino acids signals were localized on the infested side of the leaf, which suggests that metabolites leak from dead cells invoked by the aphid affection.[171] Additionally, pipecolic acid, salicylic acid, formononetin, and dihydroxyflavone were detected at the infestation site and less concentration or no target analyte was detected on the control tissue. Pipecolic acid and salicylic acid are strongly related to systemic resistance and there is higher isoflavonoid content in feeding soybean leaves.[206]

Glucosinolates are a group of metabolites synthesized by host plants against pathogens or herbivores. The glucosinolates of *Sinapis alba* L. acuminate to higher levels in hemolymph of *Athalia rosae* larvae than in the gut, as revealed by high performance liquid chromatography (HPLC) analysis[212] (Figure 8(a)). Utilizing a direct and visualized method, MALDI-IMS was used to scan the section of *A. rosae* larvae feeding on the host plant at different times. The glucosinolate sinalbin was ingested by the larvae and absorbed into the hemolymph circulatory system and rarely localized in the larval gut. This result demonstrates that IMS can support research on the distribution of plant secondary metabolites ingested by insects and the mechanisms of insecticides.

Animal–Microbe Interactions

Animals, including humans, are the most widely studied targets of IMS. Although many studies that involve IMS have been conducted with animals, cases of interactions with microbes are still rare and also mostly related to proteomics. The importance of small molecules in animal–microbe interactions is underestimated especially in the fields of ecology, medicine, and pharmacy.

Gut microbiota are crucial to the health of their animal host. Many bacteria have their own niches and interact with host tissue and neighboring microbes. The metabolites produced by microbiota are considered to play a role in transmission factors, some of which are known. IMS has also been used in unknown metabolite discovery related to gut microbiota. An important case conducted by Rath et al. used NanoDESI to identify the metabolites inside mouse gut fed with *Bacteroides thetaiotaomicron* or both *B. thetaiotaomicron* and *Bidobacterium longum*[213] (Figure 8(b)). Then MALDI-IMS was used to track the target metabolites in the mouse gut tissue sections. Several glycans, polar metabolites, and cholesterol-derived lipids were found in different gut microbiota with various expression levels.[178] This study suggested that some small molecules may be suitable for use as biomarkers of gut health and also showed that IMS can be useful in the study of small and complicated biological systems *in situ*.

IMS can also be applied to uncover chemical information about animal fungal diseases. Several species of North American bat are threatened by white-nose syndrome (WNS) which is caused by the psychrophilic fungal pathogen *Pseudogymnoascus destructans* that colonizes on the bat wings. The infection sites of *P. destructans* were revealed by microscopy AIMS (nanoDESI source), which demonstrated the metabolic differences on the surface of the healthy and infected bats.[214] The molecular networking analysis deduced from LC-MS/MS of *P. destructans* extract suggested that the secreted siderophores are crucial components of fungal growth and virulence. Furthermore, MALDI-IMS confirmed the siderophores desferrichrome, and triacetylfusarinine C were released from or located in *P. destructans* colonies. In this case, nanoDESI constitutes another option for studying the vital metabolites on the animal surface without any sample pretreatment.

Other Crucial Interactions—Mature IMS Methods, New Horizons

Recently, studies of IMS in biological research have increased; however, most works have focused on single species, clinical, and animal tissue sections. Cross-species IMS application is still not a mainstream approach. Excluding microbe–microbe and plan–microbe interactions, few studies have been published; nonetheless, a lot of interaction research of high value does not include IMS and metabolomics data. Below, we outline some cases of interactions that have importance in agriculture and that we believe are worth studying using IMS techniques.

Plant–Nematode Interactions

About 14% of plant diseases of economically important crops are estimated to be caused by nematodes.[215] Compared to fungal diseases, the pathogenic mechanisms and parasite-host metabolomics of nematodes remain little studied. To our knowledge, the only IMS data about a crop-

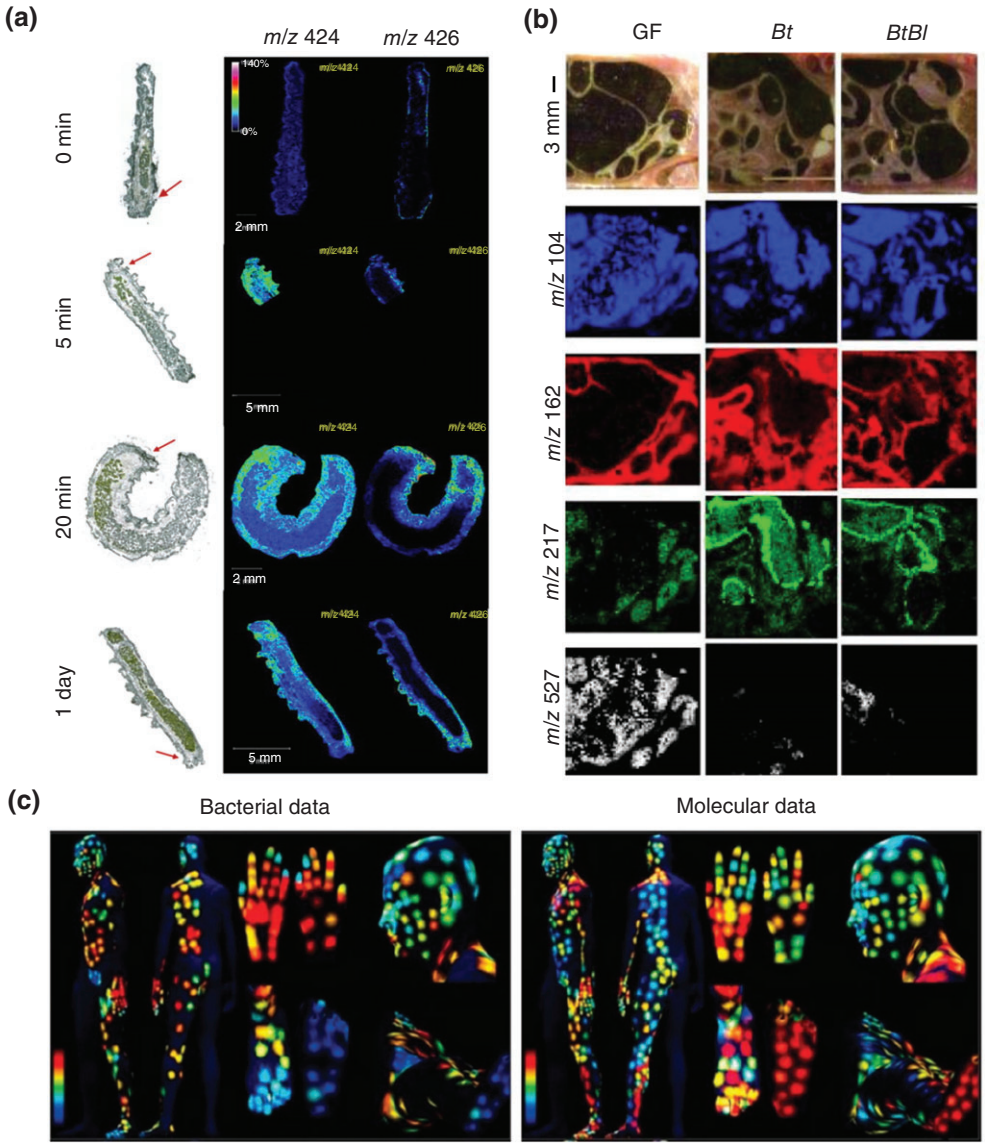

FIGURE 8 | Application of imaging mass spectrometry (IMS) to plant–insect interactions, mouse gut, and human surface microbiota. (a) Glucosinolate sinalbin (m/z 424) and an unknown metabolite (m/z 426) from Sinapis alba L. leaves were ingested by Athalia rosae larvae. IMS revealed the distribution of glucosinolate sinalbin and unknown metabolite inside the larvae after ingestion for 0 min, 5 min, 20 min, and 1 day. The intensity scales are represented as color-coded relative intensities. (b) IMS of gut microbiota in germ-free (GF), monoassociated Bacteroides thetaiotaomicron (Bt), and biassociated B. thetaiotaomicron plus Bifidobacterium longum (BtBl) mice. From top to bottom, representative metabolites are: choline (m/z 104), carnitine (m/z 217), sodiated hexuronix acid, and sodiated trihexose (m/z 527). (c) Representation of the microbial and molecular diversity of human (male) skin. Bacterial data reveals the microbial diversity according to 16S rRNA amplicon and molecular profiles were measured and identified by UPLC-QTOF-MS. For the color scale, blue represents the minimum value and red represents the maximum value. (Reprinted with permission from Refs 212. Copyright 2014 Elsevier Ltd. (a), 213. Copyright 2012 American Chemical Society (b), and 217. Copyright 2015 National Academy of Sciences (c))

nematode interaction is banana burrowing nematode disease, caused by *Radopholus similis*, which causes tremendous damage to banana crops worldwide. When LDI-IMS was employed on the lesion sites of the banana roots, multiple secondary metabolites, identified as phenylphenalenone-type phytoalexins, were found located at the lesion.[191] One of phenylphenalenones, anigorufone, showed strong motility against *R. similis*, and through the LDI-IMS analysis, it was found that ingested anigorufone was located inside yellow oil droplets. Following this workflow, we can explore the key metabolites and their functions involved in the interactions between hosts and nematodes (such as *Meloidogyne*,

Heterodera, *Pratylenchus*, etc). Furthermore, we can gain more knowledge to develop safer and more efficient nematocides.

Plant–Virus Interactions

Plant viruses are another pathogen that threatens economic crops. Viral protein particles, nucleotides, and polymerase are the main components of viruses, which are not related to secondary metabolites. However, plants produce some metabolites that can strengthen resistance at the inoculated leaf to limit the virus transference and some metabolites can induce systemic acquired resistance to defend against virus spread to other tissues. Utilizing IMS is a strategy through which visualizations of antivirus weapons can be obtained. Moreover, many kinds of plant viruses are transmitted by insect vectors such as aphids, leafhoppers, thrips, and so forth. The research workflow can also follow or coordinate with plant–insect interaction research.

Parasitic Plant–Host Plant Interactions

Dodder is a widely distributed parasitic higher plant and it can encircle, and climb on the plant host and then send a haustorium into the stem and suck nutrients from the host. The offense/defense at the interface not only includes physical attack but also chemical reactions. Until now, there has been no overall metabolomics research in this area. IMS may uncover the metabolites involved in the parasite–host plant interaction and give us hints about how to apply metabolites to eliminate dodder.

Microbe–Insect Interactions

For insects, microbes may be either symbiotic or parasitic and the study of these two relationships has different significance with regard to possible applications. As an example of the symbiotic relationship, beewolf digger wasps cultivate the symbiotic *S. philanthi*, which synthesizes and secretes several antibiotics protecting larvae cocoons against the insect pathogen.[182,216] Applying LDI-IMS, three major antibiotics, piericidin A1, piericidin B1, and streptochlorin were revealed on the surface of cocoon, forming a chemical barrier layer. The value of this symbiotic microbe for humans is that it protects beneficial insects like honeybee maintaining the production of honey. In contrast, the study of parasitic microbes is to understand how to control the pest population in the field through biocontrol agents. *Bacillus thuringiensis*, *Beauveria bassiana*, *Metarhizium anisopliae*, *Paecilomyces farinosus*, and *Nuclear polyhedrosis virus* are insect pathogens and some of them are commercialized worldwide. We believe these interaction topics have potential, and are suitable for the employment of the IMS technique to uncover the interaction of metabolites between the host and parasite.

Human Microbiota

Human skin contacts complex environmental materials all the time, and plenty of small molecules are derived from skin cells, air, and microbiota. In addition, the fluctuation of microbiota is also influenced by environment. However, it is difficult to utilize histopathology methods to support general IMS to observe the metabolomics of skin microbiota. Bouslimani et al. adopted a substitutive strategy through which molecules and microbes were collected by swabs and extracts were analyzed by UPLC-MS/MS[217] (Figure 8(c)). Like IMS data mapped on 2D images, the analyzed MS data was marked on the surface of 3D human model. Moreover, 16S rRNA data was present on the 3D model which also indicated that microbiota are correlated with metabolite distribution. This strategy is not a traditional IMS workflow, but offers similar visualization on living human skin. Expanding this 3D mapping method to animals and plants may represent a breakthrough in the exploration of the small molecules of microbiota.

CONCLUSIONS AND FUTURE PROSPECTS

IMS has been a powerful methodology for monitoring small molecules *in situ* for more than a decade. IMS provides insights to connect phenotype to chemotype by revealing the spatial distribution and structural information about molecules. This efficiently strengthens the studies of various biological interactions. Continual development and improvement in IMS instrumentation, sample preparation, analytical workflow, and software are still crucial. Metabolic identification in IMS experiments is always a bottleneck step. Besides utilizing high-resolution analyzers, ion mobility separation would be another ideal method to reinforce the molecular isolation before entrance into the analyzer. The MS and tandem data deduced from IMS techniques can be analyzed using many databases and tools. This enormous analysis work should rely on information science to trim off abundant known structures in MS and tandem MS data if we intend to discover new molecules. On the other hand, the quantitative approaches of IMS also present advantages due to visualization. How to further reduce bias in IMS data is highly depending on sample preparation and

computational approach to data analysis. Coupling multiple imaging systems also reveals multiple perspectives of targets. Sample preparation, interfaces for instrumental operation, and data analysis need to be optimized for various purposes. Uncovering the novel and complex biological interaction systems at the small molecule level represents a niche for an IMS-based workflow. Through sustained progress in development of IMS, we can expect the technique to become a powerful 'looking-glass' through which to observe the world of small molecules.

ACKNOWLEDGMENTS

We appreciate Prof. Cheng-Chih, Hsu (Department of Chemistry, National Taiwan University) for suggestion and article editing. This work was supported by grants from Ministry of Science and Technology in Taiwan (MOST 104-2320-B-001-019-MY2 to Yu-Liang Yang and MOST 104-2321-B-001-060-MY3 to Ying-Ning Ho).

FURTHER READING

Two e-books on IMS detail the principles of IMS techniques and offer useful tips on the processing of IMS:
Mass Spectrometry Imaging of Small Molecules. DOI: 10.1007/978-1-4939-1357-2. This book provides detailed principles of high vacuum and ambient MS systems and step-by-step operational information from sample preprocessing to analysis of MS data step by step.

Imaging Mass Spectrometry—Protocols for Mass Microscopy. DOI: 10.1007/978-4-431-09425-8. This book provides detailed principles of MALDI-IMS and related technical providing step-by-step information from several kinds of sample preparation methods to IMS data analysis step by step.

REFERENCES

1. Westermann AJ, Gorski SA, Vogel J. Dual RNA-seq of pathogen and host. *Nat Rev Microbiol* 2012, 10:618–630.
2. Kawahara Y, Oono Y, Kanamori H, Matsumoto T, Itoh T, Minami E. Simultaneous RNA-seq analysis of a mixed transcriptome of rice and blast fungus interaction. *PLoS One* 2012, 7:e49423.
3. Camilios-Neto D, Bonato P, Wassem R, Tadra-Sfeir MZ, Brusamarello-Santos LC, Valdameri G, Donatti L, Faoro H, Weiss VA, Chubatsu LS. Dual RNA-seq transcriptional analysis of wheat roots colonized by *Azospirillum brasilense* reveals up-regulation of nutrient acquisition and cell cycle genes. *BMC Genomics* 2014, 15:378.
4. Trim PJ, Snel MF. Small molecule MALDI MS imaging: current technologies and future challenges. *Methods* 2016, 104:127–141.
5. Sekula J, Niziol J, Rode W, Ruman T. Silver nanostructures in laser desorption/ionization mass spectrometry and mass spectrometry imaging. *Analyst* 2015, 140:6195–6209.
6. Crecelius AC, Schubert US, von Eggeling F. MALDI mass spectrometric imaging meets "omics": recent advances in the fruitful marriage. *Analyst* 2015, 140:5806–5820.
7. Wu C, Dill AL, Eberlin LS, Cooks RG, Ifa DR. Mass spectrometry imaging under ambient conditions. *Mass Spectrom Rev* 2013, 32:218–243.
8. Laskin J, Lanekoff I. Ambient mass spectrometry imaging using direct liquid extraction techniques. *Anal Chem* 2016, 88:52–73.
9. Longuespee R, Casadonte R, Kriegsmann M, Pottier C, Picard de Muller G, Delvenne P, Kriegsmann J, De Pauw E. MALDI mass spectrometry imaging: a cutting-edge tool for fundamental and clinical histopathology. *Proteomics Clin Appl* 2016, 10:701–719.
10. Yalcin EB, de la Monte SM. Review of matrix-assisted laser desorption ionization-imaging mass spectrometry for lipid biochemical histopathology. *J Histochem Cytochem* 2015, 63:762–771.
11. Schubert KO, Weiland F, Baune BT, Hoffmann P. The use of MALDI-MSI in the investigation of psychiatric and neurodegenerative disorders: a review. *Proteomics* 2016, 16:1747–1758.
12. Bowrey HE, Anderson DM, Pallitto P, Gutierrez DB, Fan J, Crouch RK, Schey KL, Ablonczy Z. Imaging mass spectrometry of the visual system: advancing the molecular understanding of retina degenerations. *Proteomics Clin Appl* 2016, 10:391–402.

13. Liu X, Hummon AB. Mass spectrometry imaging of therapeutics from animal models to three-dimensional cell cultures. *Anal Chem* 2015, 87:9508–9519.

14. Kwon HJ, Kim Y, Sugihara Y, Baldetorp B, Welinder C, Watanabe K, Nishimura T, Malm J, Torok S, Dome B, et al. Drug compound characterization by mass spectrometry imaging in cancer tissue. *Arch Pharm Res* 2015, 38:1718–1727.

15. Dong Y, Li B, Aharoni A. More than pictures: when MS imaging meets histology. *Trends Plant Sci* 2016, 21:686–698.

16. Sturtevant D, Lee YJ, Chapman KD. Matrix assisted laser desorption/ionization-mass spectrometry imaging (MALDI-MSI) for direct visualization of plant metabolites *in situ*. *Curr Opin Biotechnol* 2016, 37:53–60.

17. Dong Y, Li B, Malitsky S, Rogachev I, Aharoni A, Kaftan F, Svatos A, Franceschi P. Sample preparation for mass spectrometry imaging of plant tissues: a review. *Front Plant Sci* 2016, 7:60.

18. Boughton BA, Thinagaran D, Sarabia D, Bacic A, Roessner U. Mass spectrometry imaging for plant biology: a review. *Phytochem Rev* 2016, 15:445–488.

19. Luzzatto-Knaan T, Melnik AV, Dorrestein PC. Mass spectrometry tools and workflows for revealing microbial chemistry. *Analyst* 2015, 140:4949–4966.

20. Shih CJ, Chen PY, Liaw CC, Lai YM, Yang YL. Bringing microbial interactions to light using imaging mass spectrometry. *Nat Prod Rep* 2014, 31:739–755.

21. Yang JY, Phelan VV, Simkovsky R, Watrous JD, Trial RM, Fleming TC, Wenter R, Moore BS, Golden SS, Pogliano K, et al. Primer on agar-based microbial imaging mass spectrometry. *J Bacteriol* 2012, 194:6023–6028.

22. Hoshi T, Kudo M. High resolution static SIMS imaging by time of flight SIMS. *Appl Surf Sci* 2003, 203:818–824.

23. Liu WT, Yang YL, Xu YQ, Lamsa A, Haste NM, Yang JY, Ng J, Gonzalez D, Ellermeier CD, Straight PD, et al. Imaging mass spectrometry of intraspecies metabolic exchange revealed the cannibalistic factors of *Bacillus subtilis*. *Proc Natl Acad Sci USA* 2010, 107:16286–16290.

24. de Laorden CL, Beloqui A, Yate L, Calvo J, Puigivila M, Llop J, Reichardt NC. Nanostructured indium tin oxide slides for small-molecule profiling and imaging mass spectrometry of metabolites by surface-assisted laser desorption ionization MS. *Anal Chem* 2015, 87:431–440.

25. Bluestein BM, Morrish F, Graham DJ, Guenthoer J, Hockenbery D, Porter PL, Gamble LJ. An unsupervised MVA method to compare specific regions in human breast tumor tissue samples using ToF-SIMS. *Analyst* 2016, 141:1947–1957.

26. Gulin AA, Pavlyukov MS, Gularyan SK, Nadtochenko VA. Spatial distribution of Pt^{+} ions in cisplatin-treated glioblastoma cells by time-of-flight secondary ion mass spectrometry. *Biol Membrany* 2015, 32:202–210.

27. Van Nuffel S, Parmenter C, Scurr DJ, Russell NA, Zelzer M. Multivariate analysis of 3D ToF-SIMS images: method validation and application to cultured neuronal networks. *Analyst* 2016, 141:90–95.

28. Vaidyanathan S, Fletcher JS, Lockyer NP, Vickerman JC. TOF-SIMS investigation of *Streptomyces coelicolor*, a mycelial bacterium. *Appl Surf Sci* 2008, 255:922–925.

29. Geier FM, Fearn S, Bundy JG, McPhail DS. ToF-SIMS analysis of biomolecules in the model organism *Caenorhabditis elegans*. *Surf Interface Anal* 2013, 45:234–236.

30. Passarelli MK, Newman CF, Marshall PS, West A, Gilmore IS, Bunch J, Alexander MR, Dollery CT. Single-Cell Analysis: visualizing pharmaceutical and metabolite uptake in cells with label-free 3D mass spectrometry imaging. *Anal Chem* 2015, 87:6696–6702.

31. Peukert M, Matros A, Lattanzio G, Kaspar S, Abadia J, Mock HP. Spatially resolved analysis of small molecules by matrix-assisted laser desorption/ionization mass spectrometric imaging (MALDI-MSI). *New Phytol* 2012, 193:806–815.

32. Wang JN, Qiu SL, Chen SM, Xiong CQ, Liu HH, Wang JY, Zhang N, Hou J, He Q, Nie ZX. MALDI-TOF MS imaging of metabolites with a N-(1-Naphthyl) ethylenediamine dihydrochloride matrix and its application to colorectal cancer liver metastasis. *Anal Chem* 2015, 87:422–430.

33. Yang YL, Xu YQ, Straight P, Dorrestein PC. Translating metabolic exchange with imaging mass spectrometry. *Nat Chem Biol* 2009, 5:885–887.

34. Yang YL, Xu YQ, Kersten RD, Liu WT, Meehan MJ, Moore BS, Bandeira N, Dorrestein PC. Connecting chemotypes and phenotypes of cultured marine microbial assemblages by imaging mass spectrometry. *Angew Chem Int Ed* 2011, 50:5839–5842.

35. Holscher D, Shroff R, Knop K, Gottschaldt M, Crecelius A, Schneider B, Heckel DG, Schubert US, Svatos A. Matrix-free UV-laser desorption/ionization (LDI) mass spectrometric imaging at the single-cell level: distribution of secondary metabolites of *Arabidopsis thaliana* and *Hypericum* species. *Plant J* 2009, 60:907–918.

36. Sluszny C, Yeung ES, Nikolau BJ. *In situ* probing of the biotic-abiotic boundary of plants by laser desorption/ionization time-of-flight mass spectrometry. *J Am Soc Mass Spectrom* 2005, 16:107–115.

37. McLean JA, Stumpo KA, Russell DH. Size-selected (2–10 nm) gold nanoparticles for matrix assisted laser desorption ionization of peptides. *J Am Chem Soc* 2005, 127:5304–5305.

38. Chen CT, Chen YC. Fe_3O_4/TiO_2 core/shell nanoparticles as affinity probes for the analysis of phosphopeptides using TiO_2 surface-assisted laser desorption/ionization mass spectrometry. *Anal Chem* 2005, 77:5912–5919.
39. Chiang CK, Chen WT, Chang HT. Nanoparticle-based mass spectrometry for the analysis of biomolecules. *Chem Soc Rev* 2011, 40:1269–1281.
40. Su CL, Tseng WL. Gold nanoparticles as assisted matrix for determining neutral small carbohydrates through laser desorption/ionization time-of-flight mass spectrometry. *Anal Chem* 2007, 79:1626–1633.
41. Jurchen JC, Rubakhin SS, Sweedler JV. MALDI-MS imaging of features smaller than the size of the laser beam. *J Am Soc Mass Spectrom* 2005, 16:1654–1659.
42. Zavalin A, Todd EM, Rawhouser PD, Yang JH, Norris JL, Caprioli RM. Direct imaging of single cells and tissue at sub-cellular spatial resolution using transmission geometry MALDI MS. *J Mass Spectrom* 2012, 47:1473–1481.
43. Rompp A, Schafer KC, Guenther S, Wang Z, Kostler M, Leisner A, Paschke C, Schramm T, Spengler B. High-resolution atmospheric pressure infrared laser desorption/ionization mass spectrometry imaging of biological tissue. *Anal Bioanal Chem* 2013, 405:6959–6968.
44. Shrestha B, Patt JM, Vertes A. *In situ* cell-by-cell imaging and analysis of small cell populations by mass spectrometry. *Anal Chem* 2011, 83:2947–2955.
45. Chen Y, Liu Y, Allegood J, Wang E, Cachon-Gonzalez B, Cox TM, Merrill AH Jr, Sullards MC. Imaging MALDI mass spectrometry of sphingolipids using an oscillating capillary nebulizer matrix application system. *Methods Mol Biol* 2010, 656:131–146.
46. Anderton CR, Chu RK, Tolic N, Creissen A, Pasa-Tolic L. Utilizing a robotic sprayer for high lateral and mass resolution MALDI FT-ICR MSI of microbial cultures. *J Am Soc Mass Spectrom* 2016, 27:556–559.
47. Vergeiner S, Schafferer L, Haas H, Muller T. Improved MALDI-TOF microbial mass spectrometry imaging by application of a dispersed solid matrix. *J Am Soc Mass Spectrom* 2014, 25:1498–1501.
48. Hoffmann T, Dorrestein PC. Homogeneous matrix deposition on dried agar for MALDI imaging mass spectrometry of microbial cultures. *J Am Soc Mass Spectrom* 2015, 26:1959–1962.
49. Goodwin RJ, MacIntyre L, Watson DG, Scullion SP, Pitt AR. A solvent-free matrix application method for matrix-assisted laser desorption/ionization imaging of small molecules. *Rapid Commun Mass Spectrom* 2010, 24:1682–1686.
50. Hankin JA, Barkley RM, Murphy RC. Sublimation as a method of matrix application for mass spectrometric imaging. *J Am Soc Mass Spectrom* 2007, 18:1646–1652.
51. Bouschen W, Schulz O, Eikel D, Spengler B. Matrix vapor deposition/recrystallization and dedicated spray preparation for high-resolution scanning microprobe matrix-assisted laser desorption/ionization imaging mass spectrometry (SMALDI-MS) of tissue and single cells. *Rapid Commun Mass Spectrom* 2010, 24:355–364.
52. Dekker LJM, van Kampen JJA, Reedijk ML, Burgers PC, Gruters RA, Osterhaus ADME, Luider TM. A mass spectrometry based imaging method developed for the intracellular detection of HIV protease inhibitors. *Rapid Commun Mass Spectrom* 2009, 23:1183–1188.
53. Guo S, Wang YM, Zhou D, Li ZL. Electric field-assisted matrix coating method enhances the detection of small molecule metabolites for mass spectrometry imaging. *Anal Chem* 2015, 87:5860–5865.
54. Chen SM, Zheng HZ, Wang JN, Hou J, He Q, Liu HH, Xiong CQ, Kong XL, Nie ZX. Carbon nanodots as a matrix for the analysis of low-molecular-weight molecules in both positive- and negative-ion matrix-assisted laser desorption/ionization time-of-flight mass spectrometry and quantification of glucose and uric acid in real samples. *Anal Chem* 2013, 85:6646–6652.
55. Chen SM, Chen L, Wang JN, Hou J, He Q, Liu JA, Wang JY, Xiong SX, Yang GQ, Nie ZX. 2,3,4,5-Tetrakis (3 ′,4 ′-dihydroxylphenyl) thiophene: a new matrix for the selective analysis of low molecular weight amines and direct determination of creatinine in urine by MALDI-TOF MS. *Anal Chem* 2012, 84:10291–10297.
56. He Q, Chen SM, Wang JN, Hou J, Wang JY, Xiong SX, Nie ZX. 1-Naphthylhydrazine hydrochloride: a new matrix for the quantification of glucose and homogentisic acid in real samples by MALDI-TOF MS. *Clin Chim Acta* 2013, 420:94–98.
57. Chen R, Chen SM, Xiong CQ, Ding XL, Wu CC, Chang HC, Xiong SX, Nie ZX. N-(1-Naphthyl) ethylenediamine dinitrate: a new matrix for negative ion MALDI-TOF MS analysis of small molecules. *J Am Soc Mass Spectrom* 2012, 23:1454–1460.
58. Liu HH, Chen R, Wang JY, Chen SM, Xiong CQ, Wang JN, Hou J, He Q, Zhang N, Nie ZX, et al. 1,5-Diaminonaphthalene hydrochloride assisted laser desorption/ionization mass spectrometry imaging of small molecules in tissues following focal cerebral ischemia. *Anal Chem* 2014, 86:10114–10121.
59. Shroff R, Rulisek L, Doubsky J, Svatos A. Acid-base-driven matrix-assisted mass spectrometry for targeted metabolomics. *Proc Natl Acad Sci USA* 2009, 106:10092–10096.
60. Thomas A, Charbonneau JL, Fournaise E, Chaurand P. Sublimation of new matrix candidates for high spatial resolution imaging mass spectrometry of lipids: enhanced information in both positive and

negative polarities after 1,5-Diaminonapthalene deposition. *Anal Chem* 2012, 84:2048–2054.

61. Potocnik NO, Porta T, Becker M, Heeren RMA, Ellis SR. Use of advantageous, volatile matrices enabled by next-generation high-speed matrix-assisted laser desorption/ionization time-of-flight imaging employing a scanning laser beam. *Rapid Commun Mass Spectrom* 2015, 29:2195–2203.
62. Najam-ul-Haq M, Rainer M, Huck CW, Hausberger P, Kraushaar H, Bonn GK. Nanostructured diamond-like carbon on digital versatile disc as a matrix-free target for laser desorption/ionization mass spectrometry. *Anal Chem* 2008, 80:7467–7472.
63. Liu R, Liu JF, Zhou XX, Jiang GB. Cysteine modified small ligament Au nanoporous film: an easy fabricating and highly efficient surface-assisted laser desorption/ionization substrate. *Anal Chem* 2011, 83:3668–3674.
64. Phan NTN, Mohammadi AS, Pour MD, Ewing AG. Laser desorption ionization mass spectrometry imaging of drosophila brain using matrix sublimation versus modification with nanoparticles. *Anal Chem* 2016, 88:1734–1741.
65. Rowell F, Hudson K, Seviour J. Detection of drugs and their metabolites in dusted latent fingermarks by mass spectrometry. *Analyst* 2009, 134:701–707.
66. Tang HW, Lu W, Che CM, Ng KM. Gold nanoparticles and imaging mass spectrometry: double imaging of latent fingerprints. *Anal Chem* 2010, 82:1589–1593.
67. Ronci M, Rudd D, Guinan T, Benkendorff K, Voelcker NH. Mass spectrometry imaging on porous silicon: investigating the distribution of bioactives in marine mollusc tissues. *Anal Chem* 2012, 84:8996–9001.
68. Tata A, Montemurro C, Porcari AM, Silva KC, de Faria JBL, Eberlin MN. Spatial distribution of theobromine—a low MW drug—in tissues via matrix-free NALDI-MS imaging. *Drug Test Anal* 2014, 6:949–952.
69. Shrivas K, Hayasaka T, Sugiura Y, Setou M. Method for simultaneous imaging of endogenous low molecular weight metabolites in mouse brain using TiO_2 nanoparticles in nanoparticle-assisted laser desorption/ionization-imaging mass spectrometry. *Anal Chem* 2011, 83:7283–7289.
70. Rudd D, Benkendorff K, Voelcker NH. Solvent separating secondary metabolites directly from biosynthetic tissue for surface-assisted laser desorption ionization mass spectrometry. *Mar Drugs* 2015, 13:1410–1431.
71. Louie KB, Bowen BP, McAlhany S, Huang YR, Price JC, Mao JH, Hellerstein M, Northen TR. Mass spectrometry imaging for *in situ* kinetic histochemistry. *Sci Rep* 2013, 3:1656.
72. Louie KB, Bowen BP, Cheng XL, Berleman JE, Chakraborty R, Deutschbauer A, Arkin A, Northen TR. "Replica-extraction-transfer" nanostructure-initiator mass spectrometry imaging of acoustically printed bacteria. *Anal Chem* 2013, 85:10856–10862.
73. Yanes O, Woo HK, Northen TR, Oppenheimer SR, Shriver L, Apon J, Estrada MN, Potchoiba MJ, Steenwyk R, Manchester M, et al. Nanostructure initiator mass spectrometry: tissue imaging and direct biofluid analysis. *Anal Chem* 2009, 81:2969–2975.
74. Lee DY, Bowen BP, Northen TR. Mass spectrometry-based metabolomics, analysis of metabolite-protein interactions, and imaging. *Biotechniques* 2010, 49:557–+.
75. Lee KH, Chiang CK, Lin ZH, Chang HT. Determining enediol compounds in tea using surface-assisted laser desorption/ionization mass spectrometry with titanium dioxide nanoparticle matrices. *Rapid Commun Mass Spectrom* 2007, 21:2023–2030.
76. Lorkiewicz P, Yappert MC. Titania microparticles and nanoparticles as matrixes for *in vitro* and *in situ* analysis of small molecules by MALDI-MS. *Anal Chem* 2009, 81:6596–6603.
77. Chen WY, Chen YC. Affinity-based mass spectrometry using magnetic iron oxide particles as the matrix and concentrating probes for SALDI MS analysis of peptides and proteins. *Anal Bioanal Chem* 2006, 386:699–704.
78. Kawasaki H, Yonezawa T, Watanabe T, Arakawa R. Platinum nanoflowers for surface-assisted laser desorption/ionization mass spectrometry of biomolecules. *J Phys Chem C* 2007, 111:16278–16283.
79. Goodwin RJA, Pitt AR, Harrison D, Weidt SK, Langridge-Smith PRR, Barrett MP, Mackay CL. Matrix-free mass spectrometric imaging using laser desorption ionisation Fourier transform ion cyclotron resonance mass spectrometry. *Rapid Commun Mass Spectrom* 2011, 25:969–972.
80. Ozawa T, Osaka I, Ihozaki T, Hamada S, Kuroda Y, Murakami T, Miyazato A, Kawasaki H, Arakawa R. Simultaneous detection of phosphatidylcholines and glycerolipids using matrix-enhanced surface-assisted laser desorption/ionization-mass spectrometry with sputter-deposited platinum film. *J Mass Spectrom* 2015, 50:1264–1269.
81. Stopka SA, Rong C, Korte AR, Yadavilli S, Nazarian J, Razunguzwa TT, Morris NJ, Vertes A. Molecular imaging of biological samples on nanophotonic laser desorption ionization platforms. *Angew Chem Int Ed* 2016, 55:4482–4486.
82. Hong M, Xu LD, Wang FL, Geng ZR, Li HB, Wang HS, Li CZ. A direct assay of carboxyl-containing small molecules by SALDI-MS on a AgNP/rGO-based nanoporous hybrid film. *Analyst* 2016, 141:2712–2726.
83. Hua X, Yu XY, Wang ZY, Yang L, Liu BW, Zhu ZH, Tucker AE, Chrisler WB, Hill EA, Thevuthasan T,

et al. *In situ* molecular imaging of a hydrated biofilm in a microfluidic reactor by ToF-SIMS. *Analyst* 2014, 139:1609–1613.

84. Park JW, Jeong H, Kang B, Kim SJ, Park SY, Kang S, Kim HK, Choi JS, Hwang D, Lee TG. Multi-dimensional TOF-SIMS analysis for effective profiling of disease-related ions from the tissue surface. *Sci Rep* 2015, 5:11077.
85. Tian H, Wucher A, Winograd N. Molecular imaging of biological tissue using gas cluster ions. *Surf Interface Anal* 2014, 46:115–117.
86. Watrous JD, Dorrestein PC. Imaging mass spectrometry in microbiology. *Nat Rev Microbiol* 2011, 9:683–694.
87. Heeren RMA, McDonnell LA, Amstalden E, Luxembourg SL, Altelaar AFM, Piersma SR. Why don't biologists use SIMS? A critical evaluation of imaging MS. *Appl Surf Sci* 2006, 252:6827–6835.
88. Altelaar AFM, Klinkert I, Jalink K, de Lange RPJ, Adan RAH, Heeren RMA, Piersma SR. Gold-enhanced biomolecular surface imaging of cells and tissue by SIMS and MALDI mass spectrometry. *Anal Chem* 2006, 78:734–742.
89. Delcorte A, Bour J, Aubriet F, Muller JF, Bertrand P. Sample metallization for performance improvement in desorption/ionization of kilodalton molecules: quantitative evaluation, imaging secondary ion MS, and laser ablation. *Anal Chem* 2003, 75:6875–6885.
90. Vanbellingen QP, Elie N, Eller MJ, Della-Negra S, Touboul D, Brunelle A. Time-of-flight secondary ion mass spectrometry imaging of biological samples with delayed extraction for high mass and high spatial resolutions. *Rapid Commun Mass Spectrom* 2015, 29:1187–1195.
91. Cooks RG, Ouyang Z, Takats Z, Wiseman JM. Detection technologies. ambient mass spectrometry. *Science* 2006, 311:1566–1570.
92. Monge ME, Harris GA, Dwivedi P, Fernandez FM. Mass spectrometry: recent advances in direct open air surface sampling/ionization. *Chem Rev* 2013, 113:2269–2308.
93. Ifa DR, Wiseman JM, Song Q, Cooks RG. Development of capabilities for imaging mass spectrometry under ambient conditions with desorption electrospray ionization (DESI). *Int J Mass Spectrom* 2007, 259:8–15.
94. Laskin J, Heath BS, Roach PJ, Cazares L, Semmes OJ. Tissue imaging using nanospray desorption electrospray ionization mass spectrometry. *Anal Chem* 2012, 84:141–148.
95. Eikel D, Vavrek M, Smith S, Bason C, Yeh S, Korfmacher WA, Henion JD. Liquid extraction surface analysis mass spectrometry (LESA-MS) as a novel profiling tool for drug distribution and metabolism analysis: the terfenadine example. *Rapid Commun Mass Spectrom* 2011, 25:3587–3596.
96. Kertesz V, Ford MJ, Van Berkel GJ. Automation of a surface sampling probe/electrospray mass spectrometry system. *Anal Chem* 2005, 77:7183–7189.
97. Chen LC, Yoshimura K, Yu Z, Iwata R, Ito H, Suzuki H, Mori K, Ariyada O, Takeda S, Kubota T. Ambient imaging mass spectrometry by electrospray ionization using solid needle as sampling probe. *J Mass Spectrom* 2009, 44:1469–1477.
98. Nemes P, Vertes A. Laser ablation electrospray ionization for atmospheric pressure, *in vivo*, and imaging mass spectrometry. *Anal Chem* 2007, 79:8098–8106.
99. Coello Y, Jones AD, Gunaratne TC, Dantus M. Atmospheric pressure femtosecond laser imaging mass spectrometry. *Anal Chem* 2010, 82:2753–2758.
100. Cheng SC, Lin YS, Huang MZ, Shiea J. Applications of electrospray laser desorption ionization mass spectrometry for document examination. *Rapid Commun Mass Spectrom* 2010, 24:203–208.
101. Takats Z, Wiseman JM, Gologan B, Cooks RG. Mass spectrometry sampling under ambient conditions with desorption electrospray ionization. *Science* 2004, 306:471–473.
102. Campbell DI, Ferreira CR, Eberlin LS, Cooks RG. Improved spatial resolution in the imaging of biological tissue using desorption electrospray ionization. *Anal Bioanal Chem* 2012, 404:389–398.
103. Li B, Knudsen C, Hansen NK, Jorgensen K, Kannangara R, Bak S, Takos A, Rook F, Hansen SH, Moller BL, et al. Visualizing metabolite distribution and enzymatic conversion in plant tissues by desorption electrospray ionization mass spectrometry imaging. *Plant J* 2013, 74:1059–1071.
104. Gerbig S, Brunn HE, Spengler B, Schulz S. Spatially resolved investigation of systemic and contact pesticides in plant material by desorption electrospray ionization mass spectrometry imaging (DESI-MSI). *Anal Bioanal Chem* 2015, 407:7379–7389.
105. Kucharikova A, Kimakova K, Janfelt C, Cellarova E. Interspecific variation in localization of hypericins and phloroglucinols in the genus *Hypericum* as revealed by desorption electrospray ionization mass spectrometry imaging. *Physiol Plant* 2016, 157:2–12.
106. Thunig J, Hansen SH, Janfelt C. Analysis of secondary plant metabolites by indirect desorption electrospray ionization imaging mass spectrometry. *Anal Chem* 2011, 83:3256–3259.
107. Muller T, Oradu S, Ifa DR, Cooks RG, Krautler B. Direct plant tissue analysis and imprint imaging by desorption electrospray ionization mass spectrometry. *Anal Chem* 2011, 83:5754–5761.
108. Mohana Kumara P, Srimany A, Ravikanth G, Uma Shaanker R, Pradeep T. Ambient ionization mass spectrometry imaging of rohitukine, a chromone anticancer alkaloid, during seed development in *Dysoxylum binectariferum* Hook.f (*Meliaceae*). *Phytochemistry* 2015, 116:104–110.

109. Cabral EC, Mirabelli MF, Perez CJ, Ifa DR. Blotting assisted by heating and solvent extraction for DESI-MS imaging. *J Am Soc Mass Spectrom* 2013, 24:956–965.

110. Watrous J, Hendricks N, Meehan M, Dorrestein PC. Capturing bacterial metabolic exchange using thin film desorption electrospray ionization-imaging mass spectrometry. *Anal Chem* 2010, 82:1598–1600.

111. Angolini CF, Vendramini PH, Araujo FD, Araujo WL, Augusti R, Eberlin MN, de Oliveira LG. Direct protocol for ambient mass spectrometry imaging on agar culture. *Anal Chem* 2015, 87:6925–6930.

112. Tata A, Perez C, Campos ML, Bayfield MA, Eberlin MN, Ifa DR. Imprint desorption electrospray ionization mass spectrometry imaging for monitoring secondary metabolites production during antagonistic interaction of fungi. *Anal Chem* 2015, 87:12298–12305.

113. Tata A, Perez CJ, Hamid TS, Bayfield MA, Ifa DR. Analysis of metabolic changes in plant pathosystems by imprint imaging DESI-MS. *J Am Soc Mass Spectrom* 2015, 26:641–648.

114. Hemalatha RG, Ganayee MA, Pradeep T. Electrospun nanofiber mats as "Smart surfaces" for desorption electrospray ionization mass spectrometry (DESI MS)-based analysis and imprint imaging. *Anal Chem* 2016, 88:5710–5717.

115. Eberlin LS, Ferreira CR, Dill AL, Ifa DR, Cheng L, Cooks RG. Nondestructive, histologically compatible tissue imaging by desorption electrospray ionization mass spectrometry. *Chembiochem* 2011, 12:2129–2132.

116. Eberlin LS, Liu X, Ferreira CR, Santagata S, Agar NY, Cooks RG. Desorption electrospray ionization then MALDI mass spectrometry imaging of lipid and protein distributions in single tissue sections. *Anal Chem* 2011, 83:8366–8371.

117. Li B, Hansen SH, Janfelt C. Direct imaging of plant metabolites in leaves and petals by desorption electrospray ionization mass spectrometry. *Int J Mass Spectrom* 2013, 348:15–22.

118. Roach PJ, Laskin J, Laskin A. Nanospray desorption electrospray ionization: an ambient method for liquid-extraction surface sampling in mass spectrometry. *Analyst* 2010, 135:2233–2236.

119. Kertesz V, Van Berkel GJ. Fully automated liquid extraction-based surface sampling and ionization using a chip-based robotic nanoelectrospray platform. *J Mass Spectrom* 2010, 45:252–260.

120. Lanekoff I, Heath BS, Liyu A, Thomas M, Carson JP, Laskin J. Automated platform for high-resolution tissue imaging using nanospray desorption electrospray ionization mass spectrometry. *Anal Chem* 2012, 84:8351–8356.

121. Haddad R, Sparrapan R, Kotiaho T, Eberlin MN. Easy ambient sonic-spray ionization-membrane interface mass spectrometry for direct analysis of solution constituents. *Anal Chem* 2008, 80:898–903.

122. Otsuka Y, Naito J, Satoh S, Kyogaku M, Hashimoto H, Arakawa R. Correction: imaging mass spectrometry of a mouse brain by tapping-mode scanning probe electrospray ionization. *Analyst* 2015, 140:1356–1358.

123. Nemes P, Barton AA, Li Y, Vertes A. Ambient molecular imaging and depth profiling of live tissue by infrared laser ablation electrospray ionization mass spectrometry. *Anal Chem* 2008, 80:4575–4582.

124. Etalo DW, De Vos RC, Joosten MH, Hall RD. Spatially resolved plant metabolomics: some potentials and limitations of laser-ablation electrospray ionization mass spectrometry metabolite imaging. *Plant Physiol* 2015, 169:1424–1435.

125. Huang MZ, Cheng SC, Jhang SS, Chou CC, Cheng CN, Shiea J, Popov IA, Nikolaev EN. Ambient molecular imaging of dry fungus surface by electrospray laser desorption ionization mass spectrometry. *Int J Mass Spectrom* 2012, 325:172–182.

126. Kononikhin A, Huang MZ, Popov I, Kostyukevich Y, Kukaev E, Boldyrev A, Spasskiy A, Leypunskiy I, Shiea J, Nikolaev E. Signal enhancement in electrospray laser desorption/ionization mass spectrometry by using a black oxide-coated metal target and a relatively low laser fluence. *Eur J Mass Spectrom* 2013, 19:247–252.

127. Shrestha B, Nemes P, Nazarian J, Hathout Y, Hoffman EP, Vertes A. Direct analysis of lipids and small metabolites in mouse brain tissue by AP IR-MALDI and reactive LAESI mass spectrometry. *Analyst* 2010, 135:751–758.

128. Creaser CS, Ratcliffe L. Atmospheric pressure matrix-assisted laser desorption/ionisation mass spectrometry: a review. *Curr Anal Chem* 2006, 2:9–15.

129. Laiko VV, Baldwin MA, Burlingame AL. Atmospheric pressure matrix assisted laser desorption/ionization mass spectrometry. *Anal Chem* 2000, 72:652–657.

130. Trimpin S, Herath TN, Inutan ED, Cernat SA, Miller JB, Mackie K, Walker JM. Field-free transmission geometry atmospheric pressure matrix-assisted laser desorption/ionization for rapid analysis of unadulterated tissue samples. *Rapid Commun Mass Spectrom* 2009, 23:3023–3027.

131. Schober Y, Guenther S, Spengler B, Rompp A. Single cell matrix-assisted laser desorption/ionization mass spectrometry imaging. *Anal Chem* 2012, 84:6293–6297.

132. Roy MC, Nakanishi H, Takahashi K, Nakanishi S, Kajihara S, Hayasaka T, Setou M, Ogawa K, Taguchi R, Naito T. Salamander retina phospholipids and their localization by MALDI imaging mass

spectrometry at cellular size resolution. *J Lipid Res* 2011, 52:463–470.

133. Perdian DC, Schieffer GM, Houk RS. Atmospheric pressure laser desorption/ionization of plant metabolites and plant tissue using colloidal graphite. *Rapid Commun Mass Spectrom* 2010, 24:397–402.
134. Jackson SN, Barbacci D, Egan T, Lewis EK, Schultz JA, Woods AS. MALDI-ion mobility mass spectrometry of lipids in negative ion mode. *Anal Methods* 2014, 6:5001–5007.
135. Li H, Smith BK, Márk L, Nemes P, Nazarian J, Vertes A. Ambient molecular imaging by laser ablation electrospray ionization mass spectrometry with ion mobility separation. *Int J Mass Spectrom* 2015, 377:681–689.
136. Prentice BM, Chumbley CW, Caprioli RM. High-speed MALDI MS/MS imaging mass spectrometry using continuous raster sampling. *J Mass Spectrom* 2015, 50:703–710.
137. Watrous J, Roach P, Alexandrov T, Heath BS, Yang JY, Kersten RD, van der Voort M, Pogliano K, Gross H, Raaijmakers JM. Mass spectral molecular networking of living microbial colonies. *Proc Natl Acad Sci USA* 2012, 109:E1743–E1752.
138. Vinaixa M, Schymanski EL, Neumann S, Navarro M, Salek RM, Yanes O. Mass spectral databases for LC/MS- and GC/MS-based metabolomics: state of the field and future prospects. *Trends Analyt Chem* 2016, 78:23–35.
139. Wang M, Carver JJ, Phelan VV, Sanchez LM, Garg N, Peng Y, Nguyen DD, Watrous J, Kapono CA, Luzzatto-Knaan T, et al. Sharing and community curation of mass spectrometry data with global natural products social molecular networking. *Nat Biotechnol* 2016, 34:828–837.
140. Allard PM, Péresse T, Bisson J, Gindro K, Marcourt L, Pham VC, Roussi F, Litaudon M, Wolfender JL. Integration of molecular networking and *in silico* MS/MS fragmentation for natural products dereplication. *Anal Chem* 2016, 88:3317–3323.
141. Duhrkop K, Shen H, Meusel M, Rousu J, Bocker S. Searching molecular structure databases with tandem mass spectra using CSI:FingerID. *Proc Natl Acad Sci USA* 2015, 112:12580–12585.
142. Bocker S, Letzel MC, Liptak Z, Pervukhin A. SIRIUS: decomposing isotope patterns for metabolite identification. *Bioinformatics* 2009, 25:218–224.
143. Sawada Y, Nakabayashi R, Yamada Y, Suzuki M, Sato M, Sakata A, Akiyama K, Sakurai T, Matsuda F, Aoki T, et al. RIKEN tandem mass spectral database (ReSpect) for phytochemicals: a plant-specific MS/MS-based data resource and database. *Phytochemistry* 2012, 82:38–45.
144. Horai H, Arita M, Kanaya S, Nihei Y, Ikeda T, Suwa K, Ojima Y, Tanaka K, Tanaka S, Aoshima K, et al. MassBank: a public repository for sharing mass spectral data for life sciences. *J Mass Spectrom* 2010, 45:703–714.
145. Wishart DS, Jewison T, Guo AC, Wilson M, Knox C, Liu Y, Djoumbou Y, Mandal R, Aziat F, Dong E. HMDB 3.0-the human metabolome database in 2013. *Nucleic Acids Res* 2012, 41:D801–D807.
146. Smith CA, O'Maille G, Want EJ, Qin C, Trauger SA, Brandon TR, Custodio DE, Abagyan R, Siuzdak G. METLIN: a metabolite mass spectral database. *Ther Drug Monit* 2005, 27:747–751.
147. Kind T, Liu KH, Lee do Y, DeFelice B, Meissen JK, Fiehn O. LipidBlast *in silico* tandem mass spectrometry database for lipid identification. *Nat Methods* 2013, 10:755–758.
148. Weber T, Blin K, Duddela S, Krug D, Kim HU, Bruccoleri R, Lee SY, Fischbach MA, Müller R, Wohlleben W. antiSMASH 3.0-a comprehensive resource for the genome mining of biosynthetic gene clusters. *Nucleic Acids Res* 2015, 43:W237–W243.
149. Medema MH, Paalvast Y, Nguyen DD, Melnik A, Dorrestein PC, Takano E, Breitling R. Pep2Path: automated mass spectrometry-guided genome mining of peptidic natural products. *PLoS Comput Biol* 2014, 10:e1003822.
150. Johnston CW, Skinnider MA, Wyatt MA, Li X, Ranieri MR, Yang L, Zechel DL, Ma B, Magarvey NA. An automated Genomes-to-Natural Products platform (GNP) for the discovery of modular natural products. *Nat Commun* 2015, 6:8421.
151. Tomlinson L, Fuchser J, Futterer A, Baumert M, Hassall DG, West A, Marshall PS. Using a single, high mass resolution mass spectrometry platform to investigate ion suppression effects observed during tissue imaging. *Rapid Commun Mass Spectrom* 2014, 28:995–1003.
152. Ellis SR, Bruinen AL, Heeren RM. A critical evaluation of the current state-of-the-art in quantitative imaging mass spectrometry. *Anal Bioanal Chem* 2014, 406:1275–1289.
153. Lietz CB, Gemperline E, Li LJ. Qualitative and quantitative mass spectrometry imaging of drugs and metabolites. *Adv Drug Deliv Rev* 2013, 65:1074–1085.
154. Chumbley CW, Reyzer ML, Allen JL, Marriner GA, Via LE, Barry CE, Caprioli RM. Absolute quantitative MALDI imaging mass spectrometry: a case of Rifampicin in liver tissues. *Anal Chem* 2016, 88:2392–2398.
155. Shroff R, Schramm K, Jeschke V, Nemes P, Vertes A, Gershenzon J, Svatos A. Quantification of plant surface metabolites by matrix-assisted laser desorption-ionization mass spectrometry imaging: glucosinolates on *Arabidopsis thaliana* leaves. *Plant J* 2015, 81:961–972.

156. Nemes P, Woods AS, Vertes A. Simultaneous imaging of small metabolites and lipids in rat brain tissues at atmospheric pressure by laser ablation electrospray ionization mass spectrometry. *Anal Chem* 2010, 82:982–988.

157. Hamm G, Bonnel D, Legouffe R, Pamelard F, Delbos JM, Bouzom F, Stauber J. Quantitative mass spectrometry imaging of propranolol and olanzapine using tissue extinction calculation as normalization factor. *J Proteomics* 2012, 75:4952–4961.158.

158. Lanekoff I, Thomas M, Carson JP, Smith JN, Timchalk C, Laskin J. Imaging nicotine in rat brain tissue by use of nanospray desorption electrospray ionization mass spectrometry. *Anal Chem* 2013, 85:882–889.

159. Vismeh R, Waldon DJ, Teffera Y, Zhao ZY. Localization and quantification of drugs in animal tissues by use of desorption electrospray ionization mass spectrometry imaging. *Anal Chem* 2012, 84:5439–5445.

160. Kallback P, Shariatgorji M, Nilsson A, Andren PE. Novel mass spectrometry imaging software assisting labeled normalization and quantitation of drugs and neuropeptides directly in tissue sections. *J Proteomics* 2012, 75:4941–4951.

161. Ràfols P, Vilalta D, Brezmes J, Cañellas N, del Castillo E, Yanes O, Ramírez N, Correig X. Signal preprocessing, multivariate analysis and software tools for MA (LDI)-TOF mass spectrometry imaging for biological applications. *Mass Spectrom Rev* 2016. doi:10.1002/mas.21527.

162. Pirman DA, Reich RF, Kiss A, Heeren RMA, Yost RA. Quantitative MALDI Tandem mass spectrometric imaging of cocaine from brain tissue with a deuterated internal standard. *Anal Chem* 2013, 85:1081–1089.

163. Nilsson A, Fehniger TE, Gustavsson L, Andersson M, Kenne K, Marko-Varga G, Andren PE. Fine mapping the spatial distribution and concentration of unlabeled drugs within tissue micro-compartments using imaging mass spectrometry. *PLoS One* 2010, 5: e11411.

164. Groseclose MR, Castellino S. A mimetic tissue model for the quantification of drug distributions by MALDI imaging mass spectrometry. *Anal Chem* 2013, 85:10099–10106.

165. Horn PJ, Silva JE, Anderson D, Fuchs J, Borisjuk L, Nazarenus TJ, Shulaev V, Cahoon EB, Chapman KD. Imaging heterogeneity of membrane and storage lipids in transgenic *Camelina sativa* seeds with altered fatty acid profiles. *Plant J* 2013, 76:138–150.

166. Attia AS, Schroeder KA, Seeley EH, Wilson KJ, Hammer ND, Colvin DC, Manier ML, Nicklay JJ, Rose KL, Gore JC, et al. Monitoring the inflammatory response to infection through the integration of MALDI IMS and MRI. *Cell Host Microbe* 2012, 11:664–673.

167. Masyuko RN, Lanni EJ, Driscoll CM, Shrout JD, Sweedler JV, Bohn PW. Spatial organization of *Pseudomonas aeruginosa* biofilms probed by combined matrix-assisted laser desorption ionization mass spectrometry and confocal Raman microscopy. *Analyst* 2014, 139:5700–5708.

168. Feenstra AD, Hansen RL, Lee YJ. Multi-matrix, dual polarity, tandem mass spectrometry imaging strategy applied to a germinated maize seed: toward mass spectrometry imaging of an untargeted metabolome. *Analyst* 2015, 140:7293–7304.

169. Seaman C, Flinders B, Eijkel G, Heeren RMA, Bricklebank N, Clench MR. "Afterlife experiment": use of MALDI-MS and SIMS imaging for the study of the nitrogen cycle within plants. *Anal Chem* 2014, 86:10071–10077.

170. Palonpon AF, Ando J, Yamakoshi H, Dodo K, Sodeoka M, Kawata S, Fujita K. Raman and SERS microscopy for molecular imaging of live cells. *Nat Protoc* 2013, 8:677–692.

171. Hell SW. Toward fluorescence nanoscopy. *Nat Biotechnol* 2003, 21:1347–1355.

172. Grinolds MS, Warner M, De Greve K, Dovzhenko Y, Thiel L, Walsworth RL, Hong S, Maletinsky P, Yacoby A. Subnanometre resolution in three-dimensional magnetic resonance imaging of individual dark spins. *Nat Nanotechnol* 2014, 9:279–284.

173. Shi XF, Liu S, Han XH, Ma J, Jiang YC, Yu GF. High-sensitivity surface-enhanced Raman scattering (sers) substrate based on a gold colloid solution with a pH Change for detection of trace-level polycyclic aromatic hydrocarbons in aqueous solution. *Appl Spectrosc* 2015, 69:574–579.

174. Shao JW, Lin MM, Li YQ, Li X, Liu JX, Liang JP, Yao HL. *In vivo* blood glucose quantification using Raman spectroscopy. *PLoS One* 2012, 7:e48127.

175. Camp CH, Cicerone MT. Chemically sensitive bioimaging with coherent Raman scattering. *Nat Photon* 2015, 9:295–305.

176. Zhang S, Joseph AA, Voit D, Schaetz S, Merboldt KD, Unterberg-Buchwald C, Hennemuth A, Lotz J, Frahm J. Real-time magnetic resonance imaging of cardiac function and flow—recent progress. *Quant Imaging Med Surg* 2014, 4:313–329.

177. Campbell RE, Tour O, Palmer AE, Steinbach PA, Baird GS, Zacharias DA, Tsien RY. A monomeric red fluorescent protein. *Proc Natl Acad Sci USA* 2002, 99:7877–7882.

178. Raman V, Artemov D, Pathak AP, Winnard PT, McNutt S, Yudina A, Bogdanov A, Bhujwalla ZM. Characterizing vascular parameters in hypoxic regions: a combined magnetic resonance and optical

imaging study of a human prostate cancer model. *Cancer Res* 2006, 66:9929–9936.

179. Chughtai K, Jiang L, Post H, Winnard PT, Greenwood TR, Raman V, Bhujwalla ZM, Heeren RMA, Glunde K. Mass spectrometric imaging of red fluorescent protein in breast tumor xenografts. *J Am Soc Mass Spectrom* 2013, 24:711–717.
180. Si T, Li B, Zhang R, Xu YR, Zhao HM, Sweedler JV. Characterization of *Bacillus subtilis* colony biofilms via mass spectrometry and fluorescence imaging. *J Proteome Res* 2016, 15:1955–1962.
181. Ong TH, Romanova EV, Roberts-Galbraith RH, Yang N, Zimmerman TA, Collins JJ, Lee JE, Kelleher NL, Newmark PA, Sweedler JV. Mass spectrometry imaging and identification of peptides associated with cephalic ganglia regeneration in *Schmidtea mediterranea*. *J Biol Chem* 2016, 291:8109–8120.
182. Kaltenpoth M, Strupat K, Svatos A. Linking metabolite production to taxonomic identity in environmental samples by (MA) LDI-FISH. *ISME J* 2016, 10:527–531.
183. Van de Plas R, Yang J, Spraggins J, Caprioli RM. Image fusion of mass spectrometry and microscopy: a multimodality paradigm for molecular tissue mapping. *Nat Methods* 2015, 12:366–372.
184. Longuespee R, Boyon C, Desmons A, Kerdraon O, Leblanc E, Farre I, Vinatier D, Day R, Fournier I, Salzet M. Spectroimmunohistochemistry: a novel form of MALDI mass spectrometry imaging coupled to immunohistochemistry for tracking antibodies. *OMICS* 2014, 18:132–141.
185. Srimany A, George C, Naik HR, Pinto DG, Chandrakumar N, Pradeep T. Developmental patterning and segregation of alkaloids in areca nut (seed of *Areca catechu*) revealed by magnetic resonance and mass spectrometry imaging. *Phytochemistry* 2016, 125:35–42.
186. Oetjen J, Aichler M, Trede D, Strehlow J, Berger J, Heldmann S, Becker M, Gottschalk M, Kobarg JH, Wirtz S, et al. MRI-compatible pipeline for three-dimensional MALDI imaging mass spectrometry using PAXgene fixation. *J Proteomics* 2013, 90:52–60.
187. Castiella A, Alústiza JM, Emparanza JI, Zapata EM, Costero B, Díez MI. Liver iron concentration quantification by MRI: are recommended protocols accurate enough for clinical practice? *Eur Radiol* 2011, 21:137–141.
188. Li Z, Chu LQ, Sweedler JV, Bohn PW. Spatial correlation of confocal Raman scattering and secondary ion mass spectrometric molecular images of lignocellulosic materials. *Anal Chem* 2010, 82:2608–2611.
189. Balat M. Production of bioethanol from lignocellulosic materials via the biochemical pathway: a review. *Energy Convers Manag* 2011, 52:858–875.
190. Lanni EJ, Masyuko RN, Driscoll CM, Dunham SJ, Shrout JD, Bohn PW, Sweedler JV. Correlated imaging with C60-SIMS and confocal Raman microscopy: visualization of cell-scale molecular distributions in bacterial biofilms. *Anal Chem* 2014, 86:10885–10891.
191. Holscher D, Dhakshinamoorthy S, Alexandrov T, Becker M, Bretschneider T, Buerkert A, Crecelius AC, De Waele D, Elsen A, Heckel DG, et al. Phenalenone-type phytoalexins mediate resistance of banana plants (*Musa* spp.) to the burrowing nematode *Radopholus similis*. *Proc Natl Acad Sci USA* 2014, 111:105–110.
192. Lanni EJ, Masyuko RN, Driscoll CM, Aerts JT, Shrout JD, Bohn PW, Sweedler JV. MALDI-guided SIMS: multiscale imaging of metabolites in bacterial biofilms. *Anal Chem* 2014, 86:9139–9145.
193. Prideaux B, ElNaggar MS, Zimmerman M, Wiseman JM, Li X, Dartois V. Mass spectrometry imaging of levofloxacin distribution in TB-infected pulmonary lesions by MALDI-MSI and continuous liquid microjunction surface sampling. *Int J Mass Spectrom* 2015, 377:699–708.
194. Traxler MF, Watrous JD, Alexandrov T, Dorrestein PC, Kolter R. Interspecies interactions stimulate diversification of the *Streptomyces coelicolor* secreted metabolome. *MBio* 2013, 4:e00459.
195. Bleich R, Watrous JD, Dorrestein PC, Bowers AA, Shank EA. Thiopeptide antibiotics stimulate biofilm formation in *Bacillus subtilis*. *Proc Natl Acad Sci USA* 2015, 112:3086–3091.
196. Liaw CC, Chen PC, Shih CJ, Tseng SP, Lai YM, Hsu CH, Dorrestein PC, Yang YL. Vitroprocines, new antibiotics against *Acinetobacter baumannii*, discovered from marine *Vibrio* sp. QWI-06 using mass-spectrometry-based metabolomics approach. *Sci Rep* 2015, 5:12856.
197. de Bruijn I, Cheng X, de Jager V, Exposito RG, Watrous J, Patel N, Postma J, Dorrestein PC, Kobayashi D, Raaijmakers JM. Comparative genomics and metabolic profiling of the genus *Lysobacter*. *BMC Genomics* 2015, 16:991.
198. Michelsen CF, Watrous J, Glaring MA, Kersten R, Koyama N, Dorrestein PC, Stougaard P. Nonribosomal peptides, key biocontrol components for *Pseudomonas fluorescens* In5, isolated from a Greenlandic suppressive soil. *MBio* 2015, 6:e00079.
199. Spraker JE, Sanchez LM, Lowe TM, Dorrestein PC, Keller NP. *Ralstonia solanacearum* lipopeptide induces chlamydospore development in fungi and facilitates bacterial entry into fungal tissues. *ISME J* 2016, 10:2317–2330.
200. Song C, Mazzola M, Cheng X, Oetjen J, Alexandrov T, Dorrestein P, Watrous J, van der Voort M, Raaijmakers JM. Molecular and chemical dialogues in bacteria-protozoa interactions. *Sci Rep* 2015, 5:12837.

201. Becker L, Carre V, Poutaraud A, Merdinoglu D, Chaimbault P. MALDI mass spectrometry imaging for the simultaneous location of resveratrol, pterostilbene and viniferins on grapevine leaves. *Molecules* 2014, 19:10587–10600.

202. Hamm G, Carre V, Poutaraud A, Maunit B, Frache G, Merdinoglu D, Muller JF. Determination and imaging of metabolites from *Vitis vinifera* leaves by laser desorption/ionisation time-of-flight mass spectrometry. *Rapid Commun Mass Spectrom* 2010, 24:335–342.

203. Pezet R, Gindro K, Viret O, Spring J-L. Glycosylation and oxidative dimerization of resveratrol are respectively associated to sensitivity and resistance of grapevine cultivars to downy mildew. *Physiol Mol Plant Path* 2004, 65:297–303.

204. Seneviratne HK, Dalisay DS, Kim KW, Moinuddin SG, Yang H, Hartshorn CM, Davin LB, Lewis NG. Non-host disease resistance response in pea (*Pisum sativum*) pods: biochemical function of DRR206 and phytoalexin pathway localization. *Phytochemistry* 2015, 113:140–148.

205. Ryffel F, Helfrich EJ, Kiefer P, Peyriga L, Portais JC, Piel J, Vorholt JA. Metabolic footprint of epiphytic bacteria on *Arabidopsis thaliana* leaves. *ISME J* 2016, 10:632–643.

206. Klein AT, Yagnik GB, Hohenstein JD, Ji Z, Zi J, Reichert MD, MacIntosh GC, Yang B, Peters RJ, Vela J, et al. Investigation of the chemical interface in the soybean-aphid and rice-bacteria interactions using MALDI-mass spectrometry imaging. *Anal Chem* 2015, 87:5294–5301.

207. Soares MS, da Silva DF, Forim MR, da Silva MF, Fernandes JB, Vieira PC, Silva DB, Lopes NP, de Carvalho SA, de Souza AA, et al. Quantification and localization of hesperidin and rutin in *Citrus sinensis* grafted on *C. limonia* after *Xylella fastidiosa* infection by HPLC-UV and MALDI imaging mass spectrometry. *Phytochemistry* 2015, 115:161–170.

208. Gemperline E, Jayaraman D, Maeda J, Ane JM, Li L. Multifaceted investigation of metabolites during nitrogen fixation in *Medicago* via high resolution MALDI-MS imaging and ESI-MS. *J Am Soc Mass Spectrom* 2015, 26:149–158.

209. Kusari S, Lamshoft M, Kusari P, Gottfried S, Zuhlke S, Louven K, Hentschel U, Kayser O, Spiteller M. Endophytes are hidden producers of maytansine in *Putterlickia* roots. *J Nat Prod* 2014, 77:2577–2584.

210. Debois D, Fernandez O, Franzil L, Jourdan E, de Brogniez A, Willems L, Clement C, Dorey S, De Pauw E, Ongena M. Plant polysaccharides initiate underground crosstalk with bacilli by inducing synthesis of the immunogenic lipopeptide surfactin. *Environ Microbiol Rep* 2015, 7:570–582.

211. Studham ME, MacIntosh GC. Multiple phytohormone signals control the transcriptional response to soybean aphid infestation in susceptible and resistant soybean plants. *Mol Plant Microbe Interact* 2013, 26:116–129.

212. Abdalsamee MK, Giampa M, Niehaus K, Muller C. Rapid incorporation of glucosinolates as a strategy used by a herbivore to prevent activation by myrosinases. *Insect Biochem Mol Biol* 2014, 52:115–123.

213. Rath CM, Alexandrov T, Higginbottom SK, Song J, Milla ME, Fischbach MA, Sonnenburg JL, Dorrestein PC. Molecular analysis of model gut microbiotas by imaging mass spectrometry and nanodesorption electrospray ionization reveals dietary metabolite transformations. *Anal Chem* 2012, 84:9259–9267.

214. Mascuch SJ, Moree WJ, Hsu CC, Turner GG, Cheng TL, Blehert DS, Kilpatrick AM, Frick WF, Meehan MJ, Dorrestein PC, et al. Direct detection of fungal siderophores on bats with white-nose syndrome via fluorescence microscopy-guided ambient ionization mass spectrometry. *PLoS One* 2015, 10: e0119668.

215. Agrios GN. *Plant pathology*, vol. 5. Burlington, MA: Elsevier Academic Press; 2005.

216. Kroiss J, Kaltenpoth M, Schneider B, Schwinger MG, Hertweck C, Maddula RK, Strohm E, Svatos A. Symbiotic Streptomycetes provide antibiotic combination prophylaxis for wasp offspring. *Nat Chem Biol* 2010, 6:261–263.

217. Bouslimani A, Porto C, Rath CM, Wang M, Guo Y, Gonzalez A, Berg-Lyon D, Ackermann G, Moeller Christensen GJ, Nakatsuji T, et al. Molecular cartography of the human skin surface in 3D. *Proc Natl Acad Sci USA* 2015, 112:E2120–2129.